Comparative transcriptomics reveals divergent paths of chitinase evolution underlying dietary convergence in ant-eating mammals

Rémi Allio, Sophie Teullet, Dave Lutgen, Amandine Magdeleine, Rachid Koual, Marie-Ka Tilak, Benoit De Thoisy, Christopher Emerling, Tristan Lefébure, Frédéric Delsuc

Comparative transcriptomics reveals divergent paths of chitinase evolution underlying dietary convergence in ant-eating mammals

Rémi Allio[1,2,§,*], Sophie Teullet[1,§], Dave Lutgen[1,3,4,§], Amandine Magdeleine[1], Rachid Koual[1], Marie-Ka Tilak[1], Benoit de Thoisy[5,6], Christopher A. Emerling[1,7], Tristan Lefébure[8], and Frédéric Delsuc[1,*]

[1]*ISEM, Univ. Montpellier, CNRS, IRD, Montpellier, France*

[2]*CBGP, INRAE, CIRAD, IRD, Montpellier SupAgro, Univ. Montpellier, Montpellier, France*

[3]*Institute of Ecology and Evolution, University of Bern, Bern, Switzerland*

[4]*Swiss ornithological Institute, Sempach, Switzerland*

[5]*Institut Pasteur de la Guyane, Cayenne, French Guiana, France*

[6]*Kwata NGO, Cayenne, French Guiana, France*

[7]*Biology Department, Reedley College, Reedley, CA, USA*

[8]*Univ. Lyon, Université Claude Bernard Lyon 1, CNRS, ENTPE, UMR 5023 LEHNA, F-69622, Villeurbanne, France*

[§]*Equal contribution*

***Correspondence**

Rémi Allio: remi.allio@inrae.fr

Frédéric Delsuc: frederic.delsuc@umontpellier.fr

Key words

Chitinases, Convergent evolution, Myrmecophagy, Mammals, Salivary glands, Transcriptomics

ORCID

Rémi Allio : 0000-0003-3885-5410
Sophie Teullet : 0000-0003-2693-1797
Dave Lutgen : 0000-0003-0793-3930
Amandine Magdeleine : NA
Rachid Koual : NA
Marie-Ka Tilak : 0000-0001-8995-3462
Benoit de Thoisy : 0000-0002-8420-5112
Christopher A. Emerling : 0000-0002-7722-7305
Tristan Lefebure : 0000-0003-3923-8166
Frédéric Delsuc : 0000-0002-6501-6287

Abstract

Ant-eating mammals represent a textbook example of convergent evolution. Among them, anteaters and pangolins exhibit the most extreme convergent phenotypes with complete tooth loss, elongated skulls, protruding tongues, hypertrophied salivary glands producing large amounts of saliva, and powerful claws for ripping open ant and termite nests. However, comparative genomic analyses have shown that anteaters and pangolins differ in their chitinase gene (*CHIA*) repertoires, which potentially degrade the chitinous exoskeletons of ingested ants and termites. While the southern tamandua (*Tamandua tetradactyla*) harbors four functional *CHIA* paralogs (*CHIA1-4*), Asian pangolins (*Manis* spp.) have only one functional paralog (*CHIA5*). Here, we performed a comparative transcriptomic analysis of salivary glands in 33 placental species, including 16 novel transcriptomes from ant-eating species and close relatives. Our results suggest that salivary glands play an important role in adaptation to an insect-based diet, as expression of different *CHIA* paralogs is observed in insectivorous species. Furthermore, convergently-evolved pangolins and anteaters express different chitinases in their digestive tracts. In the Malayan pangolin, *CHIA5* is overexpressed in all major digestive organs, whereas in the southern tamandua, all four functional paralogs are expressed, at very high levels for *CHIA1* and *CHIA2* in the pancreas, and for *CHIA3* and *CHIA4* in the salivary glands, stomach, liver, and pancreas. Overall, our results demonstrate that divergent molecular mechanisms underlie convergent adaptation to the ant-eating diet in pangolins and anteaters. This study highlights the role of historical contingency and molecular tinkering of the chitin-digestive enzyme toolkit in this classic example of convergent evolution.

Introduction

The phenomenon of evolutionary convergence is a fascinating process in which distantly related species independently acquire similar characteristics in response to the same selection pressures. A fundamental question famously illustrated by the debate between Stephen Jay Gould (Gould 2002) and Simon Conway Morris (Conway Morris 1999) resides in the relative contribution of historical contingency and evolutionary convergence in the evolution of biodiversity. While Gould (Gould 1990; 2002) argued that the evolution of species strongly depends on the characteristics inherited from their ancestors (historical contingency), Conway Morris (Conway Morris 1999) retorted that convergent evolution is one of the dominant processes leading to biodiversity evolution. Despite the huge diversity of organisms found on Earth and the numerous potential possibilities to adapt to similar conditions, the strong deterministic force of natural selection led to numerous cases of recurrent phenotypic adaptations (Losos 2011; McGhee 2011; Losos 2018). However, the role of historical contingency and evolutionary tinkering in convergent evolution has long been recognized, with evolution proceeding from available material through natural selection often leading to structural and functional imperfections (Jacob 1977). As first pointed out by François Jacob (Jacob 1977), molecular tinkering seems to be particularly frequent and has shaped the evolutionary history of a number of protein families (McGlothlin et al. 2016; Pillai et al. 2020; Xie et al. 2021). Indeed, if in some cases, convergent phenotypes can be associated with similar or identical mutations in the same genes occurring in independent lineages (Arendt and Reznick 2008), in other cases, they appear to arise by diverse molecular paths (*e.g*. Christin et al. 2010). Hence, both historical contingency and evolutionary convergence seems to have impacted the evolution of the current biodiversity and the major question relies on evaluating the relative impact of these two evolutionary processes (Blount et al. 2018).

A notable example of convergent evolution is the adaptation to the specialized ant- and/or termite-eating diet (*i.e*. myrmecophagy) in placental mammals (Reiss 2001). Within placental mammals, over 200 species include ants and termites in their regime, but only 22 of them can be considered as specialized myrmecophagous mammals, eating more than 90% of social insects (Redford 1987). Historically, based on shared morphological characteristics, ant-eating mammals were considered monophyletic (*i.e*. Edentata; Novacek 1992; O'Leary et al. 2013), but molecular phylogenetic evidence now strongly supports their polyphyly (*e.g*. Delsuc et al. 2002; Meredith et al. 2011; Springer et al. 2013). This highly-specialized diet has indeed independently evolved in five placental orders: armadillos (Cingulata), anteaters

(Pilosa), aardvarks (Tubulidentata), pangolins (Pholidota), and aardwolves (Carnivora). As a consequence of foraging for small-sized prey (Redford 1987), similar morphological adaptations have evolved in these mammalian species such as powerful claws used to dig into ant and termite nests, tooth reduction culminating in complete tooth loss in anteaters and pangolins (Ferreira-Cardoso et al. 2019), an elongated muzzle with an extensible tongue (Ferreira-Cardoso et al. 2020), and viscous saliva produced by hypertrophied salivary glands (Reiss 2001). Due to strong energetic constraints imposed by a nutritionally poor diet, myrmecophagous mammals also share relatively low metabolic rates and might thus require specific adaptations to extract nutrients from the chitinous exoskeletons of their prey (McNab 1984). It has long been shown that chitinase enzymes are present in the digestive tract of mammals and vertebrates more broadly (Jeuniaux 1961; Jeuniaux 1966; Jeuniaux 1971; Jeuniaux and Cornelius 1997). More recent studies have indeed shown that chitinase genes are present in the mammalian genome and may play an important digestive function in insectivorous species (Bussink et al. 2007; Emerling et al. 2018; Janiak et al. 2018; Wang et al. 2020; Cheng et al. 2022). Elevated levels of digestive enzyme gene expression have notably been observed in placental mammal salivary glands. For instance in bat salivary glands, studies have shown that dietary adaptations can be associated with elevated expression levels in carbohydrase, lipase, and protease genes (Francischetti et al. 2013; Phillips et al. 2014; Vandewege et al. 2020).

In placental mammals, the salivary glands are composed of three major gland pairs (parotid, sublingual, and submandibular) and hundreds of minor salivary glands (Tucker 1958). In most myrmecophagous placental lineages, it has been shown that hypertrophied submandibular salivary glands are the primary source of salivary production. These enlarged horseshoe-shaped glands extend posteriorly along the side of the neck and ventrally over the chest. In the Malayan pangolin (*Manis javanica*), recent transcriptomic (Ma et al. 2017; Ma et al. 2019) and proteomic (Zhang et al. 2019) studies have shown that genes associated with digestive enzymes are highly expressed in salivary glands, which supports the hypothesis that the enlarged submandibular glands play an important functional role in social insect digestion. This result also found support in a study on the molecular evolution of the chitinase genes across 107 placental mammals that revealed the likely existence of a repertoire of five functional paralogous chitinase (*CHIA*, acidic mammalian chitinase) genes in the placental ancestor, which was subsequently shaped through multiple pseudogenization events associated with dietary adaptation during the placental radiation (Emerling et al. 2018). The widespread gene loss observed in carnivorous and herbivorous lineages resulted in a general

positive correlation between the number of functional *CHIA* paralogs and the percentage of invertebrates in the diet across placentals (Emerling et al. 2018). Indeed, mammals with a low proportion of insects in their diet present none or a few functional *CHIA* paralogs and those with a high proportion of insects in their diet generally have retained four or five functional *CHIA* paralogs (Emerling et al. 2018; Janiak et al. 2018; Wang et al. 2020). Among mammals, pangolins appear as an exception as the two investigated species (*M. javanica* and *Manis pentadactyla*) possess only one functional *CHIA* paralog (*CHIA5*) whereas other myrmecophagous species such as the southern tamandua (*Tamandua tetradactyla*) and the aardvark (*Orycteropus afer*) possess respectively four (*CHIA1-4*) and five (*CHIA1-5*) functional paralogs (Emerling et al. 2018). The presence of the sole *CHIA5* in pangolins was interpreted as the consequence of historical contingency with the probable loss of *CHIA1-4* functionality in the last common ancestor of Pholidota and Carnivora (Emerling et al. 2018). In Carnivora, it has recently been confirmed that a non insect-based diet has caused structural and functional changes in the *CHIA* gene repertoire resulting in multiple losses of function with only few species including insects in their diet retaining a fully functional *CHIA5* gene (Tabata et al. 2022). The fact that *CHIA5* was found to be highly expressed in the main digestive organs of the Malayan pangolin (Ma et al. 2017; Ma et al. 2019; Cheng et al. 2022) suggests that pangolins might compensate for their reduced chitinase repertoire by an increased ubiquitous expression of their only remaining functional paralog in multiple organs.

To test this hypothesis, we first reconstructed the detailed evolutionary history of the chitinase gene family in mammals. Then, we conducted a comparative transcriptomic analysis of chitinase gene expression in salivary glands of 33 placental mammal species including 16 newly generated transcriptomes from myrmecophagous placentals and other mammalian species. Finally, we compared the expression of chitinase paralogs in different organs between the nine-banded armadillo (*Dasypus novemcinctus*), the Malayan pangolin (*M. javanica*), and the southern tamandua (*T. tetradactyla*) for which we produced 13 new transcriptomes from nine additional organs. Our results shed light on the molecular underpinnings of convergent evolution in ant-eating mammals by revealing that divergent paths of chitinase molecular evolution underlie dietary convergence between anteaters and pangolins.

Results

Mammalian chitinase gene family evolution

The reconciled maximum likelihood tree of mammalian chitinase genes is presented in Figure 1A. The evolution of this gene family constituted by nine paralogs is characterized by the presence of numerous inferred gene losses with 384 speciation events followed by gene loss and 48 gene duplications as estimated by the gene tree/species tree reconciliation algorithm of GeneRax. At the base of the reconciled gene tree, we found the clade *CHIA1-2/OVGP1* (optimal root inferred by the reconciliation performed with TreeRecs) followed by a duplication separating the *CHIT1/CHI3L1-2* and *CHIA3-5* groups of paralogs. Within the *CHIT1/CHI3L* clade, two consecutive duplications gave rise to *CHIT1*, then *CHI3L1* and *CHI3L2*. In the *CHIA3-5* clade, a first duplication separated *CHIA3* from *CHIA4* and *CHIA5*, which were duplicated subsequently. Marsupial *CHIA4* sequences were located at the base of the *CHIA4-5* clade suggesting that this duplication might be specific to placentals. The *CHIA5* sequences of chiropterans were found at the base of the *CHIA5* clade. The duplication that gave rise to the *CHIA4* and *CHIA5* genes appears recent and specific to eutherians (marsupials and placentals) since no other taxon was found within these clades. This scenario of chitinase gene evolution is consistent with synteny analysis showing physical proximity of *CHIA1-2* and *OVGP1* on one hand, and *CHIA3-5* on the other hand (Fig. 1B), which implies that chitinase genes evolved by successive tandem duplications. However, evidence of gene conversion between the two more recent duplicates (*CHIA4* and *CHIA5*) at least in some taxa suggests that further data are necessary to fully disentangle the origins of these two paralogs (Emerling et al. 2018). Within the *CHIA5* clade of Muroidea (Spalacidae, Cricetidae and Muridae), we found four subclades (named here *CHIA5a-d*) representing potential duplications specific to the muroid rodent species represented in our dataset. From the *CHIA5a* paralog, two consecutive duplications gave rise to the three *CHIA5b-d* paralogs represented by long branches, characterizing rapidly evolving sequences. The duplication giving rise to the *CHIA5c* and *CHIA5d* paralogs concerns only the Cricetidae and Muridae, *Nannospalax galili* (Spalacidae) being present only in the clade of the *CHIA5b* paralogous gene.

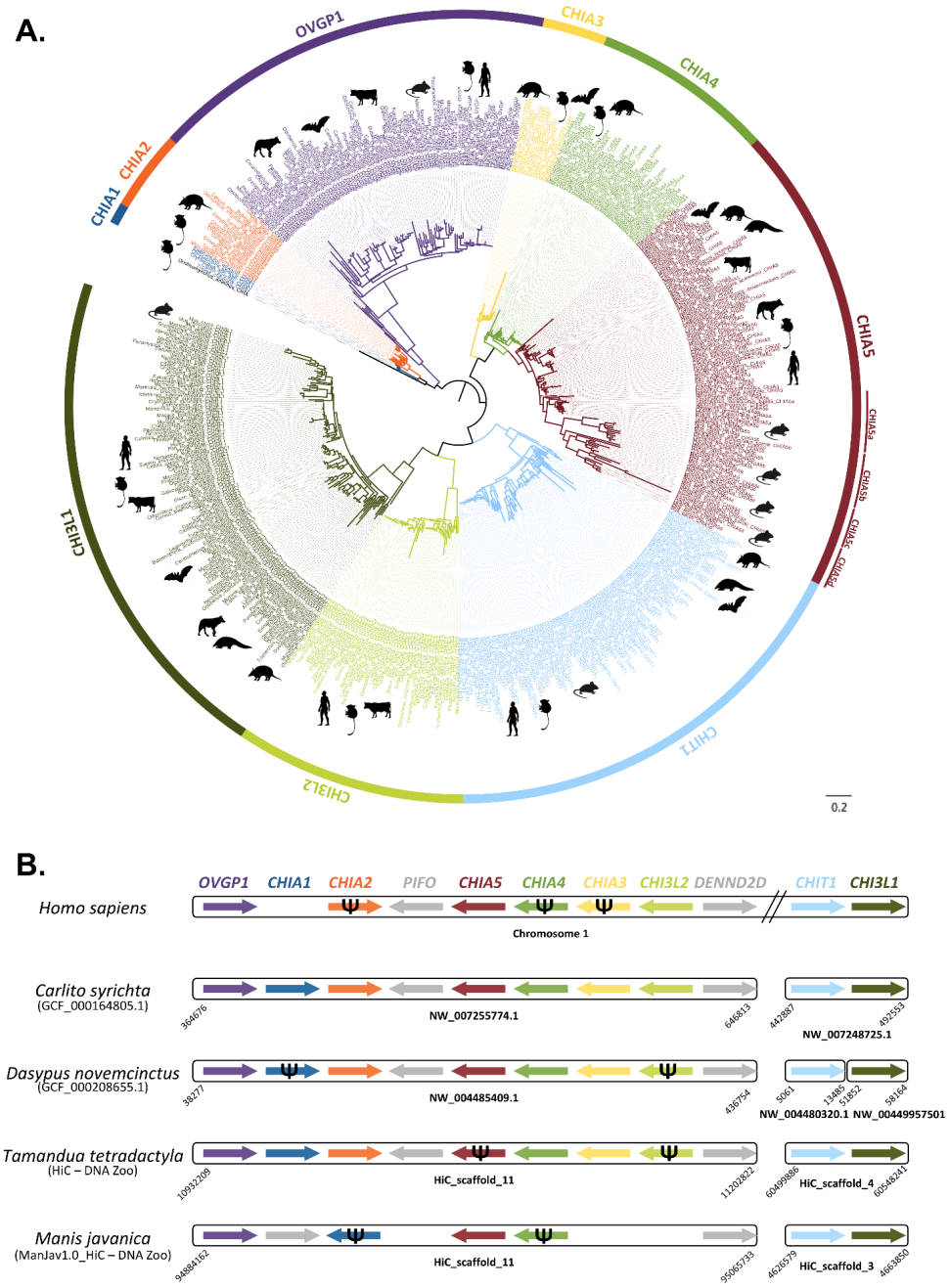

Figure 1: A. Mammalian chitinase gene family tree reconstructed using a maximum likelihood gene-tree/species-tree reconciliation approach on protein sequences. The nine chitinase paralogs are indicated on the outer circle. Scale bar represents the mean number of amino acid substitutions per site. B. Synteny of the nine chitinase paralogs in humans (*Homo sapiens*), tarsier (*Carlito syrichta*), nine-banded armadillo (*Dasypus novemcinctus*) and the two main focal convergent ant-eating species: the southern tamandua (*Tamandua tetradactyla*) and the Malayan pangolin (*Manis javanica*). Assembly names and accession numbers are indicated below species names. Arrows represent genes with scaffold/contig names and BLAST hit positions indicated below. Arrow direction indicates gene transcription direction as inferred in Genomicus v100.01 (Nguyen et al. 2022) for genes located on short contigs. Ψ symbols indicate pseudogenes as determined in Emerling et al. (2018). Genes with negative BLAST results were not represented and are probably not functional or absent.

Ancestral sequences comparison

The ancestral amino acid sequences of the nine chitinase paralogs have been reconstructed from the reconciled mammalian gene tree and compared to gain further insight into the potential function of the enzymes they encode (Fig. 2). The alignment of predicted amino acid sequences locates the chitinolytic domain between positions 133 and 140 with the preserved pattern DXXDXDXE. The ancestral sequences of CHI3L1 and CHI3L2, as all contemporary protein sequences of these genes, have a mutated chitinolytic domain with absence of a glutamic acid at position 140 (Fig. 2A), which is the active proton-donor site necessary for chitin hydrolysis (Olland et al. 2009; Hamid et al. 2013). This indicates that the ability to degrade chitin has likely been lost before the duplication leading to CHI3L1 and CHI3L2 (Fig. 2B). It is also the case for the ancestral sequences of the muroid-specific CHIA5b-d, which thus cannot degrade chitin (data not shown). The ancestral sequence of OVGP1 also presents a mutated chitinolytic site although the glutamic acid in position 140 is present (Fig. 2A). The evolution of the different chitinases therefore seems to be related to changes in their active site. The six cysteine residues allowing the binding to chitin are found at positions 371, 418, 445, 455, 457 and 458 (Fig. 2C). The absence of one of these cysteines prevents binding to chitin (Tjoelker et al., 2000) as this is the case in the ancestral OVGP1 protein where the last four cysteine residues are changed (Fig. 2C). The other ancestral sequences present the six conserved cysteine residues and thus can bind to chitin (Fig. 2C).

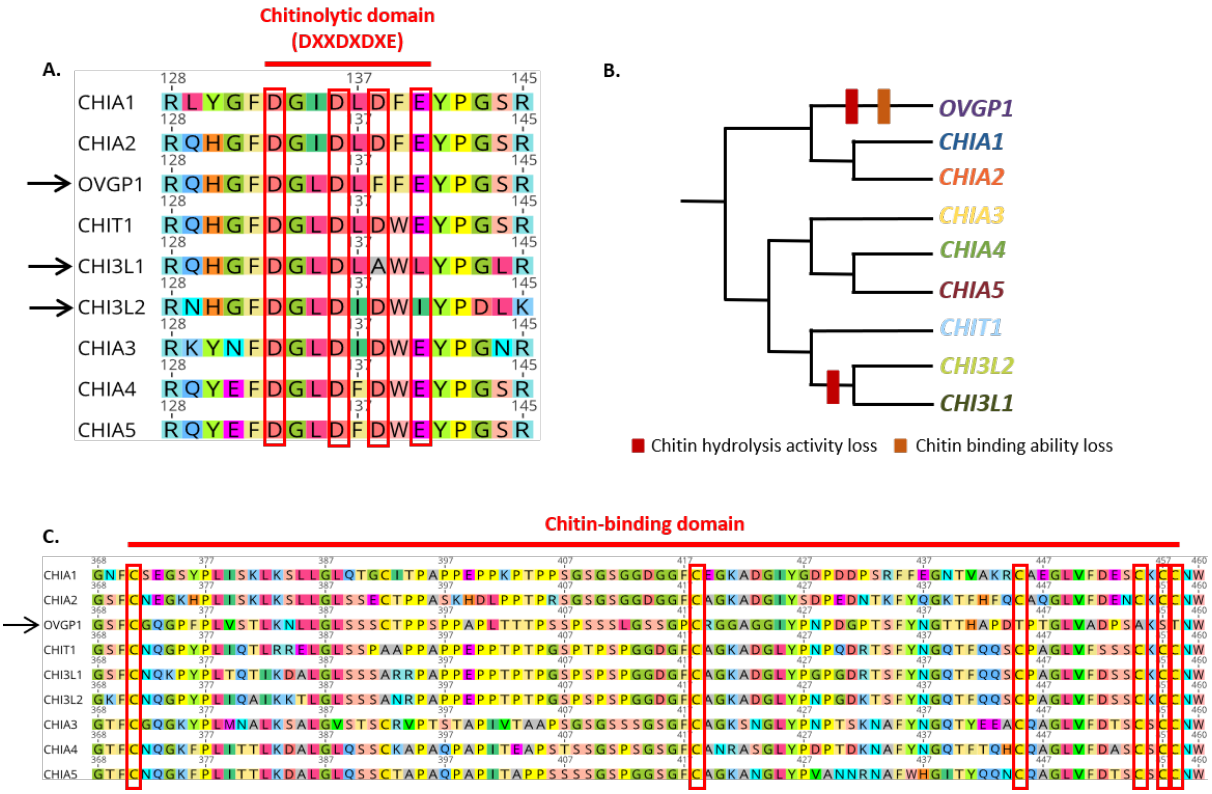

Figure 2: Comparison of predicted ancestral sequences of the nine mammalian chitinase paralogs. A. Conserved residues of the canonical chitinolytic domain active site (DXXDXDXE). Arrows indicate paralogs in which changes occurred in the active site. B. Summary of the evolution of chitinase paralogs functionality. C. Conserved cysteine residues of the chitin-binding domain. The arrow indicates OVGP1 in which the last four cysteines have been replaced.

Chitinase gene expression in mammalian salivary glands

To test the hypothesis that salivary glands play an important functional role in the digestion of ants and termites in ant-eating mammals, we analyzed the gene expression profiles of the nine chitinase paralogs revealed by the gene family tree reconstruction in 40 salivary gland transcriptomes (Fig. 3). *CHIA1* was expressed only in the elephant shrew (*Elephantulus myurus*; 23.22 normalized read counts [NC]). *CHIA2* was expressed only in the wild boar (*Sus scrofa*; 48.84 NC). *CHIA3* was expressed in the two insectivorous California leaf-nosed bats (*Macrotus californicus*; 367.70, and 35.03 NC) and in all three southern tamandua individuals (*T. tetradactyla*; 48.66, 41.52, and 15.14 NC). *CHIA4* was also highly expressed in all three southern tamandua individuals (565.61, 214.83, and 180.26 NC), in the giant anteater (*M. tridactyla*; 50.74 NC), and in the two California leaf-nosed bats (*M. californicus*; 17,224.06, and 16,880.24 NC). Expression of *CHIA5* was much higher in the two Malayan pangolin individuals (*Manis javanica*; 196,778.69 and 729.18 NC) and Thomas's nectar bat

(*Hsunycteris thomasi*; 7,301.82 NC) than in the three other species in which we detected expression of this gene: the domestic mouse (*Mus musculus*; 40.15 NC), common genet (*Genetta genetta*; 132.64 NC), and wild boar (*Sus scrofa*; 152.20 NC). *CHIT1* was expressed in many species (12 out of 40 samples) with NC values ranging from 46.76 NC in a single southern tamandua (*T. tetradactyla*) individual to 115,739.25 NC in the short-tailed shrew tenrec (*Microgale brevicaudata*). *CHI3L1* was expressed in most species (24 out of 40 samples) with values ranging from 61.68 NC in the giant anteater (*M. tridactyla*) to 1,297.01 NC in a Malayan pangolin (*M. javanica*) individual. *CHI3L2* was expressed in human (*H. sapiens*; 1334.07 NC), wild boar (*S. scrofa*; 246.41 NC), elephant shrew (*E. myurus*; 94.65 NC), and common tenrec (*Tenrec ecaudatus*; 68.62 NC). *OVGP1* was only found expressed at very low levels in domestic dog (*Canis lupus familiaris*; 6.80 NC), human (*H. sapiens*; 15.33 NC), one of the two Malayan pangolins (*M. javanica*; 4.99 NC) and wild boar (*S. scrofa*; 17.84 NC). Finally, the southern aardwolf (*P. cristatus*), Norway rat (*Rattus norvegicus*), Parnell's mustached bat (*Pteronotus parnellii*) and six phyllostomid bat species (*Carollia sowelli*, *Centurio senex*, *Glossophaga commissarisi*, *Sturnira hondurensis*, *Trachops cirrhosus*, and *Uroderma bilobatum*) did not appear to express any of the nine chitinase gene paralogs in any of our salivary gland samples.

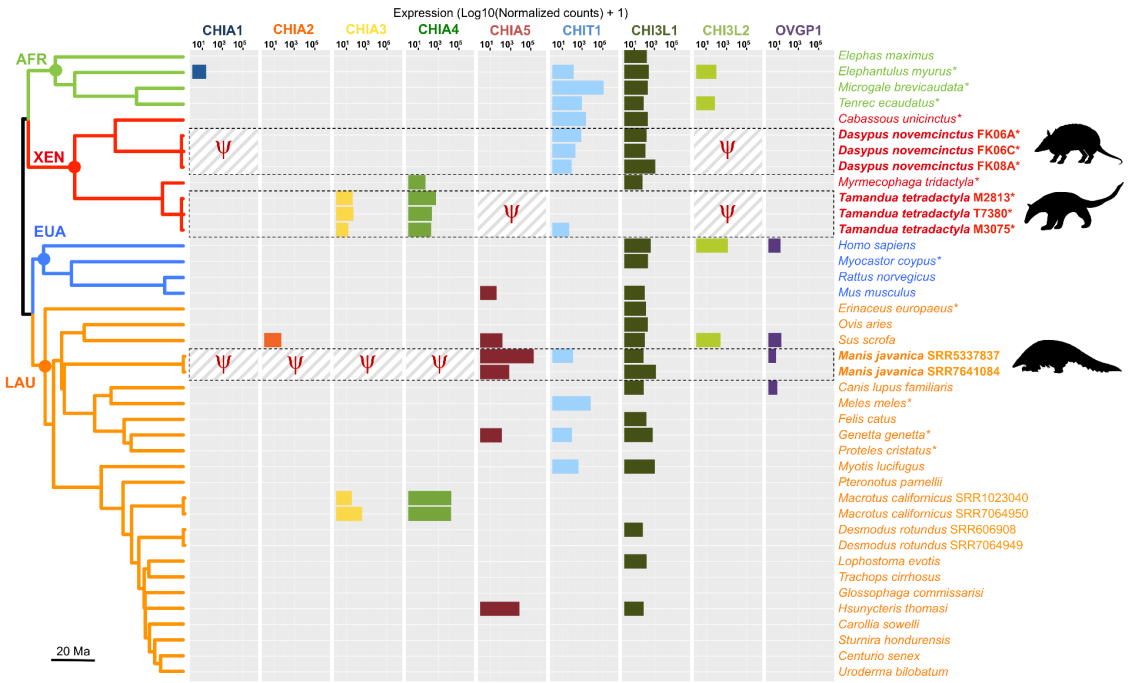

Figure 3: Comparative expression of the nine chitinase paralogs in 40 mammalian salivary gland transcriptomes. The 33 species are presented in the phylogenetic context covering the four major placental clades: Afrotheria (AFR), Xenarthra (XEN), Euarchontoglires (EUA), and Laurasiatheria (LAU). The chronogram was extracted from www.timetree.org (Kumar et

al. 2022). Non-functional pseudogenes of the three focal species (in bold) are represented by the Ψ symbol: nine-banded armadillo (*Dasypus novemcinctus*), southern tamandua (*Tamandua tetradactyla*) and Malayan pangolin (*Manis javanica*). Expression level is represented as log10 (Normalized Counts + 1). Asterisks indicate the 16 new transcriptomes produced in this study. Silhouettes were obtained from www.phylopic.org.

Chitinase gene expression in additional digestive and non-digestive organs

The expression level of the nine chitinase paralogs in several organs was compared among three species including an insectivorous xenarthran (the nine-banded armadillo; *D. novemcinctus*) and two of the main convergent myrmecophagous species (the southern anteater; *T. tetradactyla*, and the Malayan pangolin; *M. javanica*) (Fig. 4). This analysis revealed marked differences in expression level of these genes among the three species and among their digestive and non-digestive organs. *CHIT1* was expressed in all tissues in *M. javanica,* in the testes, tongue, salivary glands, and small intestine in *T. tetradactyla*, and in the cerebellum, lungs, salivary glands, and liver in *D. novemcinctus*. *CHI3L1* was found to be expressed in the majority of digestive and non-digestive tissues in all three species. *CHI3L2* is non-functional or even absent in the genome of these three species and was therefore not expressed. *OVGP1* was only weakly expressed in the lungs and salivary glands of *M. javanica* (2.22 and 4.99 NC, respectively).

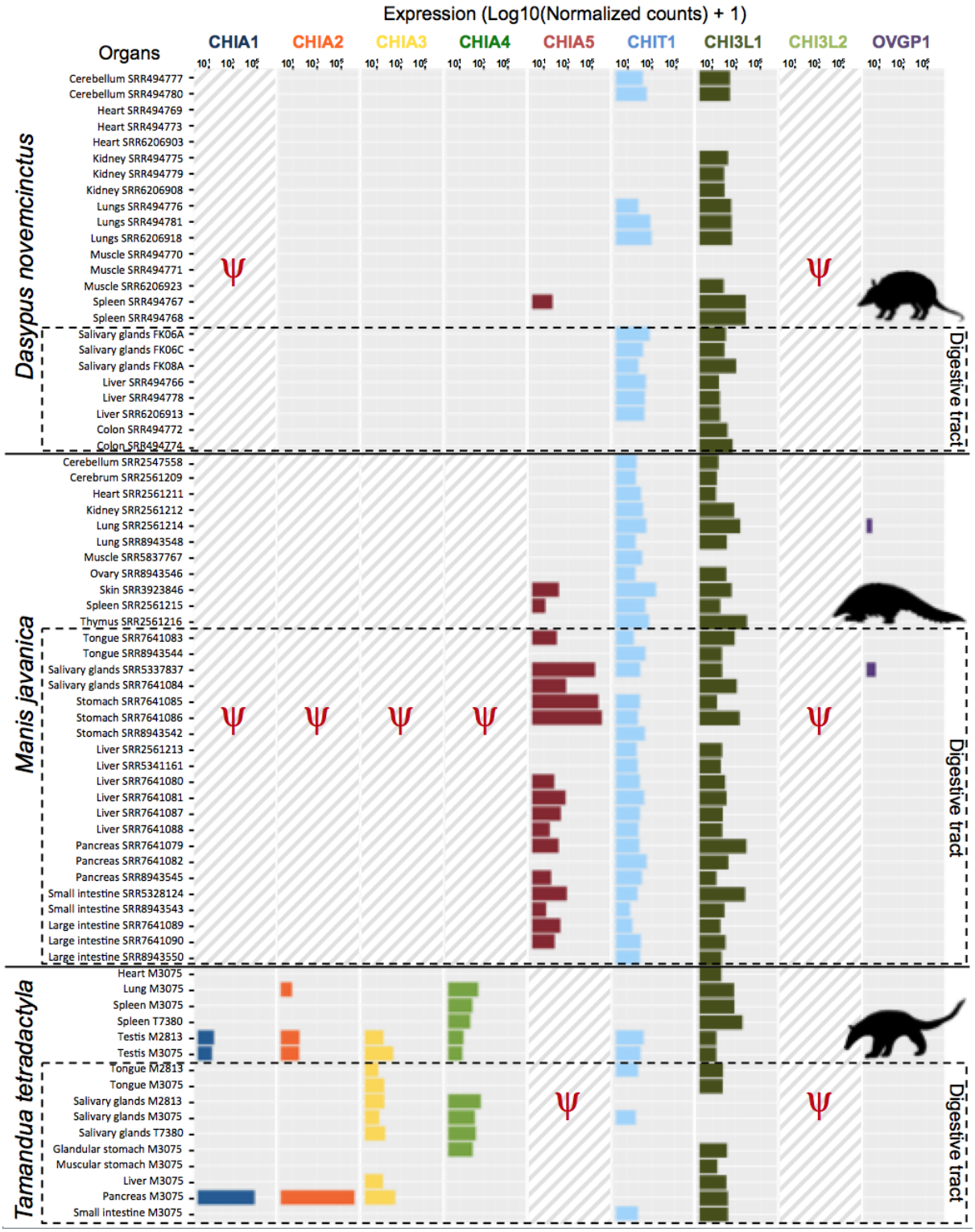

Figure 4: Comparative expression of the nine chitinase paralogs in 72 transcriptomes from different organs of the three focal species: the nine-banded armadillo (*Dasypus novemcinctus*), the Malayan pangolin (*Manis javanica*), and the southern tamandua (*Tamandua tetradactyla*). Non-functional pseudogenes are represented by the Ψ symbol and hatched background. Boxes indicate organs of the digestive tract. Expression level is represented as log10 (Normalized Counts + 1). Silhouettes were obtained from www.phylopic.org.

In the nine-banded armadillo (*D. novemcinctus*), although only *CHIA1* is pseudogenized and therefore logically not expressed, we did not detect any expression of *CHIA2*, *CHIA3*, and *CHIA4* in the tissues studied here, and *CHIA5* was only weakly expressed in one spleen sample (51.90 NC) (Fig. 4). In the Malayan pangolin (*M. javanica*), whereas *CHIA1-4* are non-functional and consequently not expressed, *CHIA5* was found expressed in all digestive organs with particularly high levels in the stomach (377,324.73 and 735,264.20 NC) and salivary glands (196,778.69 and 729.18 NC), and at milder levels in the tongue (121.24 NC), liver (254.79 NC on average when expressed), pancreas (168.64 and 39.33 NC), large intestine (238.45 and 79.32 NC), and small intestine (847.51 and 13.72 NC), but also in skin (178.95 NC) and spleen (12.06 NC) samples. Conversely, in the southern tamandua (*T. tetradactyla*), only *CHIA5* is pseudogenized and accordingly not expressed (Fig. 4). *CHIA1* was found highly expressed in the pancreas (64,443.05 NC) and weakly expressed in testes (22.74 and 14.73 NC), and *CHIA2* also had very high expression in the pancreas (1,589,834.39 NC), and low expression in testes (36.51 and 34.52 NC) and lungs (8.22 NC). *CHIA3* was also expressed in the pancreas (359.03 NC), testes (241.79 and 35.42 NC), tongue (39.53 and 12.44 NC), salivary glands (48.66, 41.52, and 15.14 NC), and liver (32.40 NC). Finally, *CHIA4* was expressed in the testes (19.48 and 14.59 NC), spleen (109.97 and 73.31 NC), lungs (340.84 NC), salivary glands (565.61, 214.83, and 180.26 NC), and glandular stomach (116.11 NC).

Discussion

Evolution of chitinase paralogs towards different functions

Chitinases have long been suggested to play an important role in mammalian insect digestion (Jeuniaux 1961; Jeuniaux 1966; Jeuniaux 1971; Jeuniaux and Cornelius 1997). Phylogenetic analyses of the Glycosyl Hydrolase gene family (GH18), which comprises genes encoding chitinase-like proteins, have revealed a dynamic evolutionary history despite a high degree of synteny among mammals (Bussink et al. 2007; Hussain and Wilson 2013). Our maximum likelihood phylogenetic analyses recovered nine functional paralogous chitinase gene sequences in mammalian genomes (Fig. 1A). In addition to the five previously characterized *CHIA* paralogs (Emerling et al. 2018; Janiak et al. 2018), we were able to identify an additional gene, *OVGP1*, which is most closely related to the previously characterized *CHIA1*

and *CHIA2* genes. In mammals, OVGP1 plays a role in fertilization and embryonic development (Buhi 2002; Saint-Dizier et al. 2014; Algarra et al. 2016; Laheri et al. 2018). However, other aliases for OVGP1 include Mucin 9 and CHIT5 (www.genecards.org) suggesting a possible digestive function. This result was further confirmed by synteny analyses suggesting a common origin by tandem duplication for *CHIA1-2* and *OVGP1* within the conserved chromosomal cluster that also includes *CHIA3-5* and *CHI3L2* (Fig. 1B). Comparison of the ancestral amino acid sequences of the nine chitinase paralogs revealed differences in their ability to bind and degrade chitin (Fig. 2), suggesting that these paralogs have evolved towards different functional specializations. The evolution of chitinase-like proteins was accompanied by a loss of enzymatic activity for chitin hydrolysis, which occurred several times independently (Bussink et al. 2007; Funkhouser and Aronson 2007; Hussain and Wilson 2013; Fig. 2B). CHI3L1 and CHI3L2, which are expressed in various cell types including macrophages and synovial cells, play roles in cell proliferation and immune response (Recklies et al. 2002; Areshkov et al. 2011; Lee et al. 2011). In contrast to these chitinase-like proteins, CHIT1 and the five CHIAs are able to degrade chitin. In humans, *CHIT1* is expressed in macrophages and neutrophils and is suspected to be involved in the defense against chitin-containing pathogens such as fungi (Gordon-Thomson et al. 2009; Lee et al. 2011). In addition to their role in chitin digestion (Boot et al. 2001), CHIAs are also suggested to play a role in the inflammatory response (Lee et al. 2011) and are expressed in non-digestive tissues, in agreement with our comparative transcriptomic results. Thus, it has been proposed that the expansion of the chitinase gene family is related to the emergence of the innate and adaptive immune systems in vertebrates (Funkhouser and Aronson 2007).

CHIA genes specific to muroid rodents and characterized by rapidly evolving sequences have also been described as chitinase-like rodent-specific (CHILrs) enzymes (Bussink et al. 2007; Hussain and Wilson 2013). These enzymes also appear to have evolved for functions in the immune response (Lee et al. 2011; Hussain and Wilson 2013). CHIA5b cannot bind to chitin, unlike CHIA5c and CHIA5d, suggesting different roles for these three paralogous proteins. The evolution of the different *CHIA1-5* genes has involved changes in their catalytic sites, which have consequences for the secondary structure of enzymes and potentially affect their optimal pH or function, as it has recently been shown for *CHIA5* in Carnivora (Tabata et al. 2022). Experimental testing of the chitin degrading activity on different substrates and at different pH of enzymes produced from the ancestral sequences reconstructed for each of the five *CHIA* paralogs would allow a better understanding of their

enzymatic activity. Studying the potential binding of these enzymes to other substrates would shed more light on their functional roles. For example, changing a cysteine in the chitin-binding domain prevents binding to this substrate but not to tri-N-acetyl-chitotriose (Tjoelker et al. 2000), a compound derived from chitin with antioxidant properties (Chen et al. 2003; Salgaonkar et al. 2015). Such functional assays, complemented by transcriptomic data to determine their expression profile in different tissues and organs (as previously done in the Malayan pangolin; Yusoff et al. 2016; Ma et al. 2017; Ma et al. 2019; Cheng et al. 2022), may help to decipher their respective roles in mammalian digestion (see below).

Impact of historical contingency and molecular tinkering on chitinase evolution and expression

In the specific case of adaptation to myrmecophagy, comparative genomic and transcriptomic analyses of these chitinase genes, particularly the chitin-degrading CHIAs, have led to a better understanding of how convergent adaptation to myrmecophagy in placentals occurs at the molecular level (Emerling et al. 2018; Cheng et al. 2022). On the one hand, anteaters (Pilosa; Vermilingua) likely inherited five *CHIA* genes from an insectivorous ancestor (Emerling et al. 2018), but then the *CHIA5* gene was lost. In the southern tamandua (*T. tetradactyla*), the inactivating mutations of *CHIA5* were identified and the estimated inactivation time of this gene was 6.8 Ma, subsequent to the origin of Vermilingua (34.2 Ma) and after the divergence with the giant anteater (*M. tridactyla*) at 11.3 Ma, suggesting a loss specific to lesser anteaters of the genus *Tamandua* (Emerling et al. 2018). In our study this gene was not found to be expressed in the salivary glands of the giant anteater. On the other hand, *CHIA5* is functional in insectivorous carnivores (Carnivora) and pangolins (Pholidota), whereas *CHIA1-4* are pseudogenized (Emerling et al. 2018; Tabata et al. 2022). Similar inactivating mutations have been observed in the *CHIA1* gene in carnivores and pangolins and dated to at least 67 Ma, well before the origin of carnivores (46.2 Ma) and pangolins (26.5 Ma) (Emerling et al. 2018). Thus, despite relying on a fully myrmecophagous diet, pangolins have only one functional *CHIA* gene, likely due to a historical contingency related to their common inheritance with carnivores. These analyses have thus revealed contrasting pseudogenization events between convergent myrmecophagous species, with lesser anteaters (genus *Tamandua*) retaining four out of the five functional chitin-degrading *CHIA* genes (*CHIA1-4*), while the Malayan pangolin (*M. javanica*) inherited only the fifth one (*CHIA5*). This peculiar evolutionary history raised the question whether the Malayan pangolin might

compensate for the paucity of its functional chitinase gene repertoire by overexpressing *CHIA5* in different digestive organs.

Since the presence of enlarged salivary glands is a hallmark of convergent ant-eating mammals, ensuring massive production of saliva to help catch and potentially digest prey, we first investigated chitinase gene expression in mammalian salivary glands. Our comparative transcriptomic study spanning a diversity of species with different diets revealed that, among ant-eating mammals, the Malayan pangolin (*M. javanica*), the southern tamandua (*T. tetradactyla*), and the giant anteater (*M. tridactyla*) all express one or more chitin-degrading genes in their salivary glands. More specifically, we found that *CHIA1* and *CHIA2* were almost never expressed in mammalian salivary glands. In contrast, *CHIA4* was found to be expressed in the giant anteater (M. tridactyla) and expression of both *CHIA3* and *CHIA4*was observed in the three southern tamandua (*T. tetradactyla*) individuals surveyed. Apart from anteaters, these two chitinase genes were found to be highly expressed only in the two individuals of the insectivorous California leaf-nosed bat (*M. californicus*), but not in any of the other 11 bat species including insectivorous species such as *M. myotis, P. parnellii, and L. evotis* (Fig. 3). . A possible explanation is that these genes have been pseudogenized in many of these bat species, which would be concordant with the findings of comparative genomic studies reporting widespread pseudogenizations of *CHIA* paralogs across multiple bat species (Emerling et al. 2018) with complete loss of *CHIA1-5* function in the vampire bat for instance (Wang et al. 2020). However, although *CHIA4* and *CHIA5* appear to be functional in the insectivorous little brown myotis (*M. lucifugus*; Emerling et al. 2018; Wang et al. 2020), we did not observe expression of these genes in the salivary gland transcriptome we analyzed. Also, *CHIA5* was found to be highly expressed in Thomas's nectar bat (*H. thomasi*). Although this bat species feeds mostly on nectar and fruits, its diet also includes a substantial part of insects suggesting that CHIA5 might play a role in chitin digestion in its salivary glands. Transcriptomic analyses of additional digestive tissues besides salivary glands in bats (Vandewege et al. 2020) may further clarify this pattern since chitinolytic activity has previously been reported in the stomachs of seven insectivorous bat species (Strobel et al. 2013). Finally, we were able to confirm the hypothesis implying an overexpression of the only functional *CHIA* gene possessed by the Malayan pangolin. Indeed, salivary gland expression profiles of *CHIA5* in *M. javanica* were much higher than in the four other species (Thomas's nectar bat, mouse, genet and wild boar) in which we detected expression of this gene, but also substantially higher than the expression of any other chitin-degrading *CHIA* in the 32 other mammalian species considered. Overall, our chitinase gene expression results

therefore support a primary role for salivary glands in insect-eating placental mammal prey digestion through the use of distinct *CHIA* paralogs (*CHIA3*, *CHIA4*, and *CHIA5*) in different species.

Our differential expression comparison of the distinct chitinase paralogs across different organs further highlighted the importance of *CHIA5* for Malayan pangolin digestive physiology by confirming its ubiquitous expression in all major tissues of the digestive tract (tongue, salivary glands, stomach, pancreas, liver, and large and small intestines) (Ma et al. 2017; Ma et al. 2019; Cheng et al. 2022; and Fig. 4). More specifically, *CHIA5* was found to be expressed at particularly high levels in the stomach and salivary glands. These results are in line with previous proteomic studies that have also identified *CHIA5* as a digestive enzyme (Zhang et al. 2019), which has been confirmed to be highly expressed by RT-qPCR in the specialized oxyntic glands of the stomach (Ma et al. 2018a; Cheng et al. 2022), reflecting a key adaptation of the Malayan pangolin to its strictly myrmecophagous diet. By contrast, in the southern tamandua (*T. tetradactyla*) only *CHIA5* is pseudogenized (Emerling et al. 2018; Cheng et al. 2022) and all functional *CHIAs* were found expressed in its digestive tract but not in the same tissues. *CHIA1* and *CHIA2* were particularly highly expressed in the pancreas whereas *CHIA3* and *CHIA4* were expressed across several other organs of the digestive tract including tongue, salivary glands, stomach, and liver (Fig. 4). *CHIA1-4* were also expressed in other non-digestive organs (testes, lungs, and spleen), but their co-expression in the salivary glands of the three distinct southern tamandua individuals sampled here (Figs. 3, 4) strongly suggests that they play a crucial role in chitin digestion in this myrmecophagous species. Conversely, in the insectivorous nine-banded armadillo (*D. novemcinctus*), although only *CHIA1* is pseudogenized (Emerling et al. 2018) and therefore not expressed, we did not detect any expression of *CHIA2*, *CHIA3*, and *CHIA4* in the tissues of the individuals studied here, including salivary glands (Figs. 3, 4), and *CHIA5* was only weakly expressed in one spleen sample (Fig. 4). Yet, chitinases could still participate in prey digestion in the nine-banded armadillo as they have been isolated from gastric tissues (Smith et al. 1998); results we could not confirm here, the liver and colon being the only additional digestive organs besides salivary glands represented in our dataset for this species. However, the comparison with the two myrmecophagous species seems to fit well with its less specialized insectivorous diet and actually further underlines the contrasted specific use of distinct *CHIA* paralogs for chitin digestion in anteaters and pangolins.

Our results demonstrate that in the case of the southern tamandua (*T. tetradactyla*) and the Malayan pangolin (*M. javanica*), two myrmecophagous species that diverged about

100 Ma ago (Meredith et al. 2011), convergent adaptation to myrmecophagy has been achieved by using paralogs of different chitinase genes to digest chitin, probably due to phylogenetic constraints leading to the loss of *CHIA1*, *CHIA2*, *CHIA3*, and *CHIA4* in the ancestor of Ferae (Carnivora and Pholidota) as suggested by Emerling et al. (2018). Pangolins and anteaters present extreme morphological adaptations including the complete loss of dentition but a detailed study of their feeding apparatus has shown that convergent tooth loss resulted in divergent structures in the internal morphology of their mandible (Ferreira-Cardoso et al. 2019). Our results combined to this observation clearly show that the evolution of convergent phenotypes in myrmecophagous mammals does not necessarily imply similar underlying mechanisms. Our study shows that historical contingency resulted in molecular tinkering (*sensu* Jacob 1977) of the chitinase gene family at both the genomic and transcriptomic levels. Working from different starting materials (*i.e.* different *CHIA* paralogs), natural selection led pangolins and anteaters to follow different paths in their adaptation to the myrmecophagous diet.

A potential complementary role of the gut microbiome?

Chitinase gene family evolution seems to have been strongly influenced by historical contingency events related to gene loss following adaptation to a specific diet (Emerling et al. 2018; Janiak et al. 2018; Chen and Zhao 2019; Tabata et al. 2022). For instance, fossil evidence showing that stem penguins primarily relied on large prey items like fish and squid has been invoked to explain the loss of all functional *CHIA* genes in all extant penguin species despite the recent specialization of some species towards a chitin-rich crustacean diet (Cole et al. 2022). One might therefore wonder why in highly specialized myrmecophagous groups which inherited a depauperate chitinase repertoire, such as pangolins and aardwolves, secondary chitinase duplications did not occur. As we demonstrated in the Malayan pangolin, one possible solution is to adjust the expression level of the remaining *CHIA5* paralog and expand its expression to multiple digestive organs. However, contrary to anteaters and pangolins, the southern aardwolf (*P. cristatus*) did not seem to express any chitinase gene in its salivary glands (Fig. 3). The presence of frameshift mutations and stop codons was inspected in all nine chitinase genes in the southern aardwolf genome (Allio et al. 2021). As expected, *CHIA1*, *CHIA2*, *CHIA3*, *CHIA4* were indeed found to be non functional, and *CHI3L2* seems to be absent from the genome of the southern aardwolf as in most members of Carnivora (Emerling et al. 2018; Tabata et al. 2022). While no inactivating mutations could

be detected in the coding sequences of *CHIA5*, *CHI3L1*, *CHIT1* or *OVGP1*, we cannot rule out the possibility that some specific mutations in regulatory elements inactivating the expression of these genes could have appeared in *P. cristatus*. However, we verified that the southern aardwolf possesses the same amino acids at positions 214 and 216 of its *CHIA5* exon 7, which control the chitinolytic activity of this chitinase, as its sister-species the striped hyena (*Hyaena hyaena*) and the other carnivore species including insects in their diet in which *CHIA5* is fully functional (Tabata et al. 2022). This intriguing result needs to be confirmed by studying the expression profiles of chitinase genes across digestive organs including the stomach in additional aardwolf specimens.

The aardwolf lineage represents the sister-group of all other hyenas (Koepfli et al. 2006; Westbury et al. 2021) from which it diverged < 10 Ma (Eizirik et al. 2010). The fossil record indicates that the adaptation of aardwolves to myrmecophagy is relatively recent (< 4 Ma; Galiano et al. 2022) and there are no clear signs of specific adaptation to an exclusive termite-based diet in the southern aardwolf genome (Westbury et al. 2021). This raises the possibility that the gut microbiome might play a key role for termite digestion in this species as suggested by results of 16S rRNA barcoding analyses of fecal samples (Delsuc et al. 2014). Aardwolves, and myrmecophagous mammals more broadly, therefore provide a model of choice for testing whether the loss of functional *CHIA* genes could be compensated by symbiotic bacteria from the gastrointestinal tract microbiota capable of degrading chitin, as previously shown in baleen whales eating krill (Sanders et al. 2015). A first metagenomic study of the fecal microbiome of the Malayan pangolin (*M. javanica*) previously identified a number of gut bacterial taxa containing chitinase genes capable of degrading chitin (Ma et al. 2018b). A more recent study has confirmed the chitin degradation potential of the Malayan pangolin gut microbiome and proposed that chitin is digested in this species by a combination of endogenous chitinolytic enzymes produced by oxyntic glands in the stomach and bacterial chitinases secreted in the colon (Cheng et al. 2022). Moreover, metagenomic data of fecal samples from captive giant anteater (*M. tridactyla*) individuals have revealed a chitin degradation potential in their gut microbiome (Cheng et al. 2022). Future genomic and metagenomic studies conducted in independent myrmecophagous mammals should allow deciphering the relative contributions of the host genome and its associated microbiome in the convergent adaptation to the myrmecophagous diet.

Material and Methods

Chitinase gene family tree reconstruction

Reconstruction of chitinase gene family evolution - The chitinase family in placental mammals appears to be composed of nine major paralogs (*CHIA1-5*, *CHIT1*, *CHI3L1*, *CHI3L2*, *OVGP1*). Mammalian sequences similar to the protein sequence of the human chitinase gene (NP_970615.2) were searched in the NCBI non-redundant protein database using BLASTP (E-value < 10). The protein sequences identified by BLASTP were then imported into Geneious Prime (Kearse et al. 2012) and aligned using MAFFT v7.450 (Katoh and Standley 2013) with the default parameters. Preliminary gene trees were then reconstructed with maximum likelihood using RAxML v8.2.11 (Stamatakis 2014) under the LG+G4 model (Le and Gascuel 2008) as implemented in Geneious Prime. From the reconstructed tree, the sequences were filtered according to the following criteria: (1) fast-evolving sequences with an E-value greater than zero and not belonging to the chitinase family were excluded; (2) in cases of multiple isoforms, only the longest was retained; (3) sequences whose length represented less than at least 50% of the total alignment length were removed; (4) in case of identical sequences from the same species the longest was kept; and (5) sequences labeled as "Hypothetical protein" and "Predicted: low quality protein" were discarded. This procedure resulted in a dataset containing 528 mammalian sequences that were realigned using MAFFT. This alignment was then cleaned up by removing sites not present in at least 50% of the sequences resulting in a total length of 460 amino acid sites. A maximum likelihood tree was then reconstructed with RAxML-NG v0.9.0 (Kozlov et al. 2019) using 10 tree searches starting from maximum parsimony trees under the LG+G8+F model. The species tree of the 143 mammal species represented in our dataset was reconstructed based on *COI* sequences extracted from the BOLD system database v4 (Ratnasingham and Hebert 2007) by searching for “Chordata” sequences in the “Taxonomy” section. Sequences were aligned using MAFFT, the phylogeny was inferred with RAxML and the topology was then adjusted manually based on the literature to correct ancient relationships. To determine the optimal rooting scheme, a rapid reconciliation between the resulting gene tree and species tree was performed using the TreeRecs reconciliation algorithm based on maximum parsimony (Comte et al. 2020) as implemented in SeaView v5.0.2 (Gouy et al. 2010). The final chitinase gene family tree was produced using the maximum likelihood gene family tree reconciliation approach implemented in GeneRax v.1.1.0 (Morel et al. 2020) using the TreeRecs reconciled tree as input (source and result

available from Zenodo). GeneRax can reconstruct duplications, losses and horizontal gene transfer events but since the latter are negligible in mammals, only gene duplications and losses have been modeled here (--rec-model UndatedDL) and the LG+G model was used.

Ancestral sequence reconstructions - Ancestral sequences of the different paralogs were reconstructed from the reconciled tree using RAxML-NG (--ancestral function, --model LG+G8+F). The sequences were then aligned in Geneious Prime with MAFFT (source and result files available from Zenodo). Given that active chitinases are characterized by a catalytic site with a conserved amino acid motif (DXXDXDXE; Olland et al. 2009; Hamid et al. 2013), this motif was compared among all available species. Additionally, the six conserved cysteine residues responsible for chitin binding (Tjoelker et al. 2000; Olland et al. 2009) were also investigated.

Chitinase gene synteny comparisons - The synteny of the nine chitinase paralogs was compared between the two focal ant-eating species in our global transcriptomic analysis (*T. tetradactyla* and *M. javanica*), an insectivorous xenarthran species (*D. novemcinctus*), an insectivorous primate species with five functional *CHIA* genes (*Carlito syrichta*) and human (*Homo sapiens*). For *H. sapiens*, synteny information was added from Emerling et al. (2018) and completed by using Genomicus v100.01 (Nguyen et al. 2022). For *C. syrichta* and *D. novemcinctus*, genome assemblies have been downloaded from the National Center for Biotechnology Information (NCBI) and from the DNA Zoo (Choo et al. 2016; Dudchenko et al. 2017) for *M. javanica* and *T. tetradactyla*. Synteny information was retrieved by blasting (*megablast*) the different CDS sequences against these assemblies. Scaffold/contig names, positions and direction of BLAST hits were retrieved to compare their synteny (source and result files available from Zenodo). Genes with negative BLAST results were considered probably not functional or absent.

Transcriptome assemblies

Salivary gland transcriptomes - Biopsies of submandibular salivary glands (Gil et al. 2018) preserved in RNAlater were obtained from the Mammalian Tissue Collection of the Institut des Sciences de l'Evolution de Montpellier (ISEM) and the JAGUARS collection for 16 individuals representing 12 placental mammal species (Table S1). Total RNA was extracted from individual salivary gland tissue samples using the RNeasy extraction kit (Qiagen, Germany). Then, RNA-seq library construction and Illumina sequencing on a HiSeq 2500

system using paired-end 2x125bp reads were conducted by the Montpellier GenomiX platform (MGX) resulting in 16 newly produced salivary gland transcriptomes. This sampling was completed with the 26 mammalian salivary gland transcriptomes available as paired-end Illumina sequencing reads in the Short Read Archive (SRA) of the NCBI as of December 15th, 2022 representing an additional 21 species (Table S1). This taxon sampling includes representatives from all major mammal superorders Afrotheria (n = 4), Xenarthra (n = 4), Euarchontoglires (n = 4), and Laurasiatheria (n = 21) and covers six different diet categories: carnivory (n = 4), frugivory and herbivory (n = 8), insectivory (n = 9), myrmecophagy (n = 5), and omnivory (n = 7) (Table S1). Four of the five lineages in which myrmecophagous mammals evolved are represented: southern aardwolf (*P. cristatus*, Carnivora), Malayan pangolin (*M. javanica*, Pholidota), southern naked-tailed armadillo (*C. unicinctus*, Cingulata), giant anteater (*M. tridactyla*, Pilosa), and southern tamandua (*T. tetradactyla*, Pilosa). Species replicates in the form of different individuals were included for the southern tamandua (*T. tetradactyla*; n = 3), the nine-banded armadillo (*D. novemcinctus*; n = 3), the Malayan pangolin (*M. javanica*; n = 2), the vampire bat (*Desmodus rotundus*; n = 2), and the California leaf-nosed bat (*Macrotus californicus*; n = 2). We unfortunately were not able to obtain fresh salivary gland samples from the aardvark (*O. afer*, Tubulidentata), the only missing myrmecophagous lineage in our sampling.

Transcriptomes from additional organs - Tissue biopsies from nine additional organs (testis, lungs, heart, spleen, tongue, pancreas, stomach, liver, and small intestine) were sampled during dissections of three roadkill individuals of southern tamandua (*T. tetradactyla*; Table S1). Total RNA extractions from these RNAlater-preserved tissues, RNA-seq library construction, and sequencing were conducted as described above resulting in 13 newly generated transcriptomes. For comparative purposes, 21 additional transcriptomes of nine-banded armadillo (*D. novemcinctus*) representing eight organs and 30 transcriptomes of Malayan pangolin (*M. javanica*) representing 16 organs were downloaded from SRA (Table S1).

Comparative transcriptomics

Transcriptome assemblies and quality control - Adapters and low quality reads were removed from raw sequencing data using fastp v0.19.6 (Chen et al. 2018) using default parameters except for the PHRED score which was defined as "--qualified_quality_phred ≥ 15", as suggested by (MacManes 2014). Then, *de novo* assembly was performed on each individual

transcriptome sample using Trinity v2.8.4 (Grabherr et al. 2011) using default parameters (result files available from Zenodo). For one individual vampire bat (*D. rotundus*), three salivary gland transcriptomes (SRR606902, SRR606908, and SRR606911) were combined to obtain a better assembly. For each of the 104 transcriptome assemblies, completeness was assessed by the presence of Benchmark Universal Single Copy Orthologs (BUSCO v5) based on a dataset of 9,226 single-copy orthologs conserved in over 90% of mammalian species (Manni et al. 2021). This pipeline was run through the gVolante web server (Nishimura et al. 2017) to evaluate the percentage of complete, duplicated, fragmented and missing single copy orthologs within each transcriptome (Table S2).

Transcriptome annotation and orthogroup inference - The 104 transcriptome assemblies were annotated following the pipeline implemented in assembly2ORF (https://github.com/ellefeg/assembly2orf). This pipeline combines evidence-based and gene-model-based predictions. First, potential transcripts of protein-coding genes are extracted based on similarity searches (BLAST) against the peptides of Metazoa found in Ensembl (Yates et al. 2020). Then, using both protein similarity and exonerate functions (Slater and Birney 2005), a frameshift correction is applied to candidate transcripts. Candidate open reading frames (ORFs) are predicted using TransDecoder (https://github.com/TransDecoder/TransDecoder) and annotated based on homology information inferred from both BLAST and Hmmscan searches. Finally, to be able to compare the transcriptomes obtained from all species, we relied on the inference of gene orthogroups. The orthogroup inference for the translated candidate ORFs was performed using OrthoFinder v2 (Emms and Kelly 2019) using FastTree (Price et al. 2010) for gene tree reconstructions. For expression analyses, orthogroups containing more than 20 copies for at least one species were discarded.

Gene expression analyses - Quantification of transcript expression was performed on Trinity assemblies with Kallisto v.0.46.1 (Bray et al. 2016) using the *align_and_estimate_abundance.pl* script provided in the Trinity suite (Grabherr et al. 2011). Kallisto relies on pseudo-alignments of the reads to search for the original transcript of a read without looking for a perfect alignment (as opposed to classical quantification by counting the reads aligned on the assembled transcriptome; Wolf 2013). Counts (raw number of mapped reads) and the Transcripts Per kilobase Million are reported (result files available from Zenodo). Based on the previously inferred orthogroups, orthogroup-level abundance

estimates were imported and summarized using tximport (Soneson et al. 2016). To minimize sequencing depth variation across samples and gene outlier effect (a few highly and differentially expressed genes may have strong and global influence on the total read count), orthogroup-level raw reads counts were normalized using the median of the ratios of observed counts using DESeq2 (Love et al. 2014) for orthogroups containing up to 20 gene copies by species.

Chitinase expression in salivary glands - The chitinase orthogroup was extracted from the orthogroups inferred by OrthoFinder2 using BLASTX with the reference chitinase database previously created. The 476 amino acid sequences composing this orthogroup were assigned to the nine chitinase orthologs (*CHIA1-5*, *CHIT1*, *CHI3L1*, *CHI3L2*, *OVGP1*) using the maximum likelihood Evolutionary Placement Algorithm implemented in RAxML-EPA (Berger et al. 2011) with the reference chitinase sequence alignment and reconciled phylogenetic tree previously inferred using GeneRax (result files available from Zenodo). This allowed excluding three additional contaminant sequences and dividing the chitinase orthogroup into nine sub-orthogroups corresponding to each chitinase paralog. To take advantage of the transcriptome-wide expression information for the expression standardization, these new orthogroups were included in the previous orthogroup-level abundance matrix estimates and the same normalization approach using DESeq2 was conducted. Finally, gene-level abundance estimates for all chitinase paralogs were extracted and compared on a log10 scale.

Data and Resource Availability

Raw RNAseq Illumina reads have been submitted to the Short Read Archive (SRA) of the National Center for Biotechnology Information (NCBI) and are available under BioProject number PRJNA909065. Transcriptome assemblies, phylogenetic datasets, corresponding trees, and other supplementary materials are available from zenodo.org (DOI: 10.5281/zenodo.7790047).

Acknowledgments

We would like to thank Hugues Parrinello (Montpellier GenomiX platform) for advice on RNAseq, Mariana Escobar Rodríguez and Gautier Debaecker for help with transcriptome assembly and annotation, and Marie Sémon for providing useful advice on RNAseq statistical

analyses. We are also indebted to Frank Knight, Mark Scherz, Miguel Vences, Andolalao Rakotoarison, Nico Avenant, Pierre-Henri Fabre, Quentin Martinez, Nathalie Delsuc, Aude Caizergues, Roxanne Schaub, Lionel Hautier, Fabien Condamine, Sérgio Ferreira-Cardoso, and François Catzeflis for their help with tissue sampling. Computational analyses benefited from the Montpellier Bioinformatics Biodiversity (MBB) platform. The JAGUARS collection is supported through a FEDER/ERDF grant attributed to Kwata NGO, funded by the European Union, the Collectivité Territoriale de Guyane, and the DEAL Guyane. This work has been supported by grants from the European Research Council (ConvergeAnt project: ERC-2015-CoG-683257) and Investissements d'Avenir of the Agence Nationale de la Recherche (CEBA: ANR-10-LABX-25-01; CEMEB: ANR-10-LABX-0004). This is contribution ISEM 2023-XXX of the Institut des Sciences de l'Evolution de Montpellier.

References

Algarra B, Han L, Soriano-Úbeda C, Avilés M, Coy P, Jovine L, Jiménez-Movilla M. 2016. The C-terminal region of OVGP1 remodels the zona pellucida and modifies fertility parameters. *Sci. Rep.* 6:32556.

Allio R, Tilak M-K, Scornavacca C, Avenant NL, Kitchener AC, Corre E, Nabholz B, Delsuc F. 2021. High-quality carnivoran genomes from roadkill samples enable comparative species delineation in aardwolf and bat-eared fox. *eLife* 10:e63167.

Arendt J, Reznick D. 2008. Convergence and parallelism reconsidered: What have we learned about the genetics of adaptation? *Trends Ecol. Evol.* 23:26–32.

Areshkov PO, Avdieiev SS, Balynska OV, LeRoith D, Kavsan VM. 2011. Two closely related human members of Chitinase-like family, CHI3L1 and CHI3L2, activate ERK1/2 in 293 and U373 cells but have the different influence on cell proliferation. *Int. J. Biol. Sci.* 8:39–48.

Berger SA, Krompass D, Stamatakis A. 2011. Performance, accuracy, and web server for evolutionary placement of short sequence reads under maximum likelihood. *Syst. Biol.* 60:291–302.

Blount ZD, Lenski RE, Losos JB. 2018. Contingency and determinism in evolution: Replaying life's tape. *Science* 362:eaam5979.

Boot RG, Blommaart EF, Swart E, Ghauharali-van der Vlugt K, Bijl N, Moe C, Place A, Aerts JM. 2001. Identification of a novel acidic mammalian chitinase distinct from chitotriosidase. *J. Biol. Chem.* 276:6770–6778.

Bray NL, Pimentel H, Melsted P, Pachter L. 2016. Near-optimal probabilistic RNA-seq quantification. *Nat. Biotechnol.* 34:525–527.

Buhi WC. 2002. Characterization and biological roles of oviduct-specific, oestrogen-dependent glycoprotein. *Reproduction* 123:355–362.

Bussink AP, Speijer D, Aerts JMFG, Boot RG. 2007. Evolution of mammalian Chitinase(-like) members of family 18 Glycosyl Hydrolases. *Genetics* 177:959–970.

Chen A-S, Taguchi T, Sakai K, Kikuchi K, Wang M-W, Miwa I. 2003. Antioxidant activities of Chitobiose and Chitotriose. *Biol. Pharm. Bull.* 26:1326–1330.

Chen S, Zhou Y, Chen Y, Gu J. 2018. fastp: an ultra-fast all-in-one FASTQ preprocessor. *Bioinformatics* 34:i884–i890.

Chen Y-H, Zhao H. 2019. Evolution of digestive enzymes and dietary diversification in birds. *PeerJ* 7:e6840.

Cheng S-C, Liu C-B, Yao X-Q, Hu J-Y, Yin T-T, Lim BK, Chen W, Wang G-D, Zhang C-L, Irwin DM, et al. 2022. Hologenomic insights into mammalian adaptations to myrmecophagy. *Natl. Sci. Rev.*:nwac174.

Choo SW, Rayko M, Tan TK, Hari R, Komissarov A, Wee WY, Yurchenko AA, Kliver S, Tamazian G, Antunes A. 2016. Pangolin genomes and the evolution of mammalian scales and immunity. *Genome Res.* 26:1312–1322.

Christin P-A, Weinreich DM, Besnard G. 2010. Causes and evolutionary significance of genetic convergence. *Trends Genet.* 26:400–405.

Cole TL, Zhou C, Fang M, Pan H, Ksepka DT, Fiddaman SR, Emerling CA, Thomas DB, Bi X, Fang Q. 2022. Genomic insights into the secondary aquatic transition of penguins. *Nat. Commun.* 13:1–13.

Comte N, Morel B, Hasić D, Guéguen L, Boussau B, Daubin V, Penel S, Scornavacca C, Gouy M, Stamatakis A, et al. 2020. Treerecs: an integrated phylogenetic tool, from sequences to reconciliations. *Bioinformatics* 36:4822–4824.

Conway Morris S. 1999. The crucible of creation: The Burgess Shale and the rise of animals. Oxford, New York: Oxford University Press

Delsuc F, Metcalf JL, Wegener Parfrey L, Song SJ, González A, Knight R. 2014. Convergence of gut microbiomes in myrmecophagous mammals. *Mol. Ecol.* 23:1301–1317.

Delsuc F, Scally M, Madsen O, Stanhope MJ, de Jong WW, Catzeflis FM, Springer MS, Douzery EJP. 2002. Molecular phylogeny of living xenarthrans and the impact of character and taxon sampling on the placental tree rooting. *Mol. Biol. Evol.* 19:1656–

1671.

Dudchenko O, Batra SS, Omer AD, Nyquist SK, Hoeger M, Durand NC, Shamim MS, Machol I, Lander ES, Aiden AP. 2017. De novo assembly of the Aedes aegypti genome using Hi-C yields chromosome-length scaffolds. *Science* 356:92–95.

Eizirik E, Murphy WJ, Koepfli K-P, Johnson WE, Dragoo JW, Wayne RK, O'Brien SJ. 2010. Pattern and timing of diversification of the mammalian order Carnivora inferred from multiple nuclear gene sequences. *Mol. Phylogenet. Evol.* 56:49–63.

Emerling CA, Delsuc F, Nachman MW. 2018. Chitinase genes (CHIAs) provide genomic footprints of a post-Cretaceous dietary radiation in placental mammals. *Sci. Adv.* 4:eaar6478.

Emms DM, Kelly S. 2019. OrthoFinder: Phylogenetic orthology inference for comparative genomics. *Genome Biol.* 20:238.

Ferreira-Cardoso S, Delsuc F, Hautier L. 2019. Evolutionary tinkering of the mandibular canal linked to convergent regression of teeth in placental mammals. *Curr. Biol.* 29:468–475.

Ferreira-Cardoso S, Fabre P-H, Thoisy B de, Delsuc F, Hautier L. 2020. Comparative masticatory myology in anteaters and its implications for interpreting morphological convergence in myrmecophagous placentals. *PeerJ* 8:e9690.

Francischetti IMB, Assumpção TCF, Ma D, Li Y, Vicente EC, Uieda W, Ribeiro JMC. 2013. The "Vampirome": Transcriptome and proteome analysis of the principal and accessory submaxillary glands of the vampire bat *Desmodus rotundus*, a vector of human rabies. *J. Proteomics* 82:288–319.

Funkhouser JD, Aronson NN. 2007. Chitinase family GH18: Evolutionary insights from the genomic history of a diverse protein family. *BMC Evol. Biol.* 7:96.

Galiano H, Tseng ZJ, Solounias N, Wang X, Zhan-Xiang Q, White S. 2022. A new aardwolf-line fossil hyena from Middle and Late Miocene deposits of Linxia Basin, Gansu, China. *Vertebr. Palasiat.* 60:81–116.

Gil F, Arencibia A, García V, Ramírez G, Vázquez JM. 2018. Anatomic and magnetic resonance imaging features of the salivary glands in the dog. *Anat. Histol. Embryol.* 47:551–559.

Gordon-Thomson C, Kumari A, Tomkins L, Holford P, Djordjevic JT, Wright LC, Sorrell TC, Moore GPM. 2009. Chitotriosidase and gene therapy for fungal infections. *Cell. Mol. Life Sci.* 66:1116–1125.

Gould SJ. 1990. Wonderful life: The Burgess Shale and the nature of history. WW Norton &

Company

Gould SJ. 2002. The Structure of Evolutionary Theory. Harvard University Press

Gouy M, Guindon S, Gascuel O. 2010. SeaView version 4: A multiplatform graphical user interface for sequence alignment and phylogenetic tree building. *Mol. Biol. Evol.* 27:221–224.

Grabherr MG, Haas BJ, Yassour M, Levin JZ, Thompson DA, Amit I, Adiconis X, Fan L, Raychowdhury R, Zeng Q, et al. 2011. Trinity: reconstructing a full-length transcriptome without a genome from RNA-Seq data. *Nat. Biotechnol.* 29:644–652.

Hamid R, Khan MA, Ahmad M, Ahmad MM, Abdin MZ, Musarrat J, Javed S. 2013. Chitinases: An update. *J. Pharm. Bioallied Sci.* 5:21–29.

Hussain M, Wilson JB. 2013. New paralogues and revised time line in the expansion of the vertebrate GH18 family. *J. Mol. Evol.* 76:240–260.

Jacob F. 1977. Evolution and tinkering. *Science* 196:1161–1166.

Janiak MC, Chaney ME, Tosi AJ. 2018. Evolution of acidic mammalian chitinase genes (CHIA) is related to body mass and insectivory in Primates. *Mol. Biol. Evol.* 35:607–622.

Jeuniaux C. 1961. Chitinase: An addition to the list of hydrolases in the digestive tract of vertebrates. *Nature* 192:135–136.

Jeuniaux C. 1966. [111] Chitinases. In: Methods in enzymology. Vol. 8. Elsevier. p. 644–650.

Jeuniaux C. 1971. On some biochemical aspects of regressive evolution in animals. In: Biochemical evolution and the origin of life. E. Schoffeniels. p. 304–313.

Jeuniaux C, Cornelius C. 1997. Distribution and activity of chitinolytic enzymes in the digestive tract of birds and mammals. In: First international conference on Chitin/Chitosan.

Katoh K, Standley DM. 2013. MAFFT multiple sequence alignment software Version 7: Improvements in performance and usability. *Mol. Biol. Evol.* 30:772–780.

Kearse M, Moir R, Wilson A, Stones-Havas S, Cheung M, Sturrock S, Buxton S, Cooper A, Markowitz S, Duran C, et al. 2012. Geneious Basic: An integrated and extendable desktop software platform for the organization and analysis of sequence data. *Bioinformatics* 28:1647–1649.

Koepfli K-P, Jenks SM, Eizirik E, Zahirpour T, Van Valkenburgh B, Wayne RK. 2006. Molecular systematics of the Hyaenidae: relationships of a relictual lineage resolved by a molecular supermatrix. *Mol. Phylogenet. Evol.* 38:603–620.

Kozlov AM, Darriba D, Flouri T, Morel B, Stamatakis A. 2019. RAxML-NG: a fast, scalable and user-friendly tool for maximum likelihood phylogenetic inference. *Bioinformatics* 35:4453–4455.

Kumar S, Suleski M, Craig JM, Kasprowicz AE, Sanderford M, Li M, Stecher G, Hedges SB. 2022. TimeTree 5: An Expanded Resource for Species Divergence Times. *Mol. Biol. Evol.* 39:msac174.

Laheri S, Ashary N, Bhatt P, Modi D. 2018. Oviductal glycoprotein 1 (OVGP1) is expressed by endometrial epithelium that regulates receptivity and trophoblast adhesion. *J. Assist. Reprod. Genet.* 35:1419–1429.

Le SQ, Gascuel O. 2008. An improved general amino acid replacement matrix. *Mol. Biol. Evol.* 25:1307–1320.

Lee CG, Da Silva CA, Dela Cruz CS, Ahangari F, Ma B, Kang M-J, He C-H, Takyar S, Elias JA. 2011. Role of chitin and Chitinase/Chitinase-like proteins in inflammation, tissue remodeling, and injury. *Annu. Rev. Physiol.* 73:479–501.

Losos JB. 2011. Convergence, adaptation, and constraint. *Evol. Int. J. Org. Evol.* 65:1827–1840.

Losos JB. 2018. Improbable destinies: Fate, chance, and the future of evolution. Riverhead Books, New York.

Love MI, Huber W, Anders S. 2014. Moderated estimation of fold change and dispersion for RNA-seq data with DESeq2. *Genome Biol.* 15:550.

Ma J-E, Jiang H-Y, Li L-M, Zhang X-J, Li G-Y, Li H-M, Jin X-J, Chen J-P. 2018. The fecal metagenomics of Malayan pangolins identifies an extensive adaptation to myrmecophagy. *Front. Microbiol.* 9:2793.

Ma J-E, Jiang H-Y, Li L-M, Zhang X-J, Li H-M, Li G-Y, Mo D-Y, Chen J-P. 2019. SMRT sequencing of the full-length transcriptome of the Sunda pangolin (*Manis javanica*). *Gene* 692:208–216.

Ma J-E, Li L-M, Jiang H-Y, Zhang X-J, Li J, Li G-Y, Chen J-P. 2018. Acidic mammalian chitinase gene is highly expressed in the special oxyntic glands of *Manis javanica*. *FEBS Open Bio* 8:1247–1255.

Ma J-E, Li L-M, Jiang H-Y, Zhang X-J, Li J, Li G-Y, Yuan L-H, Wu J, Chen J-P. 2017. Transcriptomic analysis identifies genes and pathways related to myrmecophagy in the Malayan pangolin (*Manis javanica*). *PeerJ* 5:e4140.

MacManes M. 2014. On the optimal trimming of high-throughput mRNA sequence data. *Front. Genet.* 5:13.

Manni M, Berkeley MR, Seppey M, Simão FA, Zdobnov EM. 2021. BUSCO update: Novel and streamlined workflows along with broader and deeper phylogenetic coverage for scoring of eukaryotic, prokaryotic, and viral genomes. *Mol. Biol. Evol.* 38:4647–4654.

McGhee GR. 2011. Convergent evolution: Limited forms most beautiful. MIT Press, Boston.

McGlothlin JW, Kobiela ME, Feldman CR, Castoe TA, Geffeney SL, Hanifin CT, Toledo G, Vonk FJ, Richardson MK, Brodie ED, et al. 2016. Historical contingency in a multigene family facilitates adaptive evolution of toxin resistance. *Curr. Biol.* 26:1616–1621.

McNab BK. 1984. Physiological convergence amongst ant-eating and termite-eating mammals. *J. Zool.* 203:485–510.

Meredith RW, Janečka JE, Gatesy J, Ryder OA, Fisher CA, Teeling EC, Goodbla A, Eizirik E, Simão TLL, Stadler T, et al. 2011. Impacts of the Cretaceous terrestrial revolution and KPg extinction on mammal diversification. *Science* 334:521–524.

Morel B, Kozlov AM, Stamatakis A, Szöllősi GJ. 2020. GeneRax: A tool for species-tree-aware maximum likelihood-based gene family tree inference under gene duplication, transfer, and loss. *Mol. Biol. Evol.* 37:2763–2774.

Nguyen NTT, Vincens P, Dufayard JF, Roest Crollius H, Louis A. 2022. Genomicus in 2022: Comparative tools for thousands of genomes and reconstructed ancestors. *Nucleic Acids Res.* 50:D1025–D1031.

Nishimura O, Hara Y, Kuraku S. 2017. gVolante for standardizing completeness assessment of genome and transcriptome assemblies. *Bioinformatics* 33:3635–3637.

Novacek MJ. 1992. Mammalian phylogeny: Shaking the tree. *Nature* 356:121–125.

O'Leary MA, Bloch JI, Flynn JJ, Gaudin TJ, Giallombardo A, Giannini NP, Goldberg SL, Kraatz BP, Luo Z-X, Meng J, et al. 2013. The placental mammal ancestor and the post–K-Pg radiation of placentals. *Science* 339:662–667.

Olland AM, Strand J, Presman E, Czerwinski R, Joseph-McCarthy D, Krykbaev R, Schlingmann G, Chopra R, Lin L, Fleming M, et al. 2009. Triad of polar residues implicated in pH specificity of acidic mammalian chitinase. *Protein Sci.* 18:569–578.

Phillips CJ, Phillips CD, Goecks J, Lessa EP, Sotero-Caio CG, Tandler B, Gannon MR, Baker RJ. 2014. Dietary and flight energetic adaptations in a salivary gland transcriptome of an insectivorous bat. *PLoS One* 9:e83512.

Pillai AS, Chandler SA, Liu Y, Signore AV, Cortez-Romero CR, Benesch JLP, Laganowsky A, Storz JF, Hochberg GKA, Thornton JW. 2020. Origin of complexity in haemoglobin evolution. *Nature* 581:480–485.

Price MN, Dehal PS, Arkin AP. 2010. FastTree 2--approximately maximum-likelihood trees for large alignments. *PloS One* 5:e9490.

Ratnasingham S, Hebert PDN. 2007. bold: The barcode of life data system (http://www.barcodinglife.org). *Mol. Ecol. Notes* 7:355–364.

Recklies AD, White C, Ling H. 2002. The chitinase 3-like protein human cartilage glycoprotein 39 (HC-gp39) stimulates proliferation of human connective-tissue cells and activates both extracellular signal-regulated kinase- and protein kinase B-mediated signalling pathways. *Biochem. J.* 365:119–126.

Redford KH. 1987. Ants and termites as food. In: Genoways HH, editor. Current Mammalogy. Boston, MA: Springer US. p. 349–399.

Reiss KZ. 2001. Using phylogenies to study convergence: the case of the ant-eating mammals. *Am. Zool.* 41:507–525.

Saint-Dizier M, Marnier C, Tahir MZ, Grimard B, Thoumire S, Chastant-Maillard S, Reynaud K. 2014. OVGP1 is expressed in the canine oviduct at the time and place of oocyte maturation and fertilization. *Mol. Reprod. Dev.* 81:972–982.

Salgaonkar N, Prakash D, Nawani NN, Kapadnis BP. 2015. Comparative studies on ability of N-acetylated chitooligosaccharides to scavenge reactive oxygen species and protect DNA from oxidative damage. *Indian J. Biotechnol.* 14:186–192.

Sanders JG, Beichman AC, Roman J, Scott JJ, Emerson D, McCarthy JJ, Girguis PR. 2015. Baleen whales host a unique gut microbiome with similarities to both carnivores and herbivores. *Nat. Commun.* 6:8285.

Slater GSC, Birney E. 2005. Automated generation of heuristics for biological sequence comparison. *BMC Bioinformatics* 6:31.

Smith SA, Robbins LW, Steiert JG. 1998. Isolation and characterization of a chitinase from the nine-banded armadillo, Dasypus novemcinctus. *J. Mammal.* 79:486–491.

Soneson C, Love MI, Robinson MD. 2016. Differential analyses for RNA-seq: Transcript-level estimates improve gene-level inferences. *F1000 Res.* 4:1521.

Springer MS, Meredith RW, Teeling EC, Murphy WJ. 2013. Technical comment on "The placental mammal ancestor and the post–K-Pg radiation of placentals." *Science* 341:613–613.

Stamatakis A. 2014. RAxML version 8: a tool for phylogenetic analysis and post-analysis of large phylogenies. *Bioinformatics* 30:1312–1313.

Strobel S, Roswag A, Becker NI, Trenczek TE, Encarnaçao JA. 2013. Insectivorous bats digest chitin in the stomach using acidic mammalian chitinase. *PloS One* 8:e72770.

Tabata E, Itoigawa A, Koinuma T, Tayama H, Kashimura A, Sakaguchi M, Matoska V, Bauer PO, Oyama F. 2022. Noninsect-based diet leads to structural and functional changes of Acidic Chitinase in Carnivora. *Mol. Biol. Evol.* 39:msab331.

Tjoelker LW, Gosting L, Frey S, Hunter CL, Le Trong H, Steiner B, Brammer H, Gray PW. 2000. Structural and functional definition of the human chitinase chitin-binding domain. *J. Biol. Chem.* 275:514–520.

Tucker R. 1958. Taxonomy of the salivary glands of vertebrates. *Syst. Biol.* 7:74–83.

Vandewege MW, Sotero-Caio CG, Phillips CD. 2020. Positive selection and gene expression analyses from salivary glands reveal discrete adaptations within the ecologically diverse bat family Phyllostomidae. *Genome Biol. Evol.* 12:1419–1428.

Wang K, Tian S, Galindo-González J, Dávalos LM, Zhang Y, Zhao H. 2020. Molecular adaptation and convergent evolution of frugivory in Old World and neotropical fruit bats. *Mol. Ecol.* 29:4366–4381.

Westbury MV, Le Duc D, Duchêne DA, Krishnan A, Prost S, Rutschmann S, Grau JH, Dalén L, Weyrich A, Norén K, et al. 2021. Ecological specialization and evolutionary reticulation in extant Hyaenidae. *Mol. Biol. Evol.* 38:3884–3897.

Wolf JBW. 2013. Principles of transcriptome analysis and gene expression quantification: an RNA-seq tutorial. *Mol. Ecol. Resour.* 13:559–572.

Xie VC, Pu J, Metzger BP, Thornton JW, Dickinson BC. 2021. Contingency and chance erase necessity in the experimental evolution of ancestral proteins. *eLife* 10:e67336.

Yates AD, Achuthan P, Akanni W, Allen James, Allen Jamie, Alvarez-Jarreta J, Amode MR, Armean IM, Azov AG, Bennett R, et al. 2020. Ensembl 2020. *Nucleic Acids Res.* 48:D682–D688.

Yusoff AM, Tan TK, Hari R, Koepfli K-P, Wee WY, Antunes A, Sitam FT, Rovie-Ryan JJ, Karuppannan KV, Wong GJ. 2016. De novo sequencing, assembly and analysis of eight different transcriptomes from the Malayan pangolin. *Sci. Rep.* 6:1–11.

Zhang F, Xu N, Yu Y, Wu S, Li S, Wang W. 2019. Expression profile of the digestive enzymes of *Manis javanica* reveals its adaptation to diet specialization. *ACS Omega* 4:19925–19933.

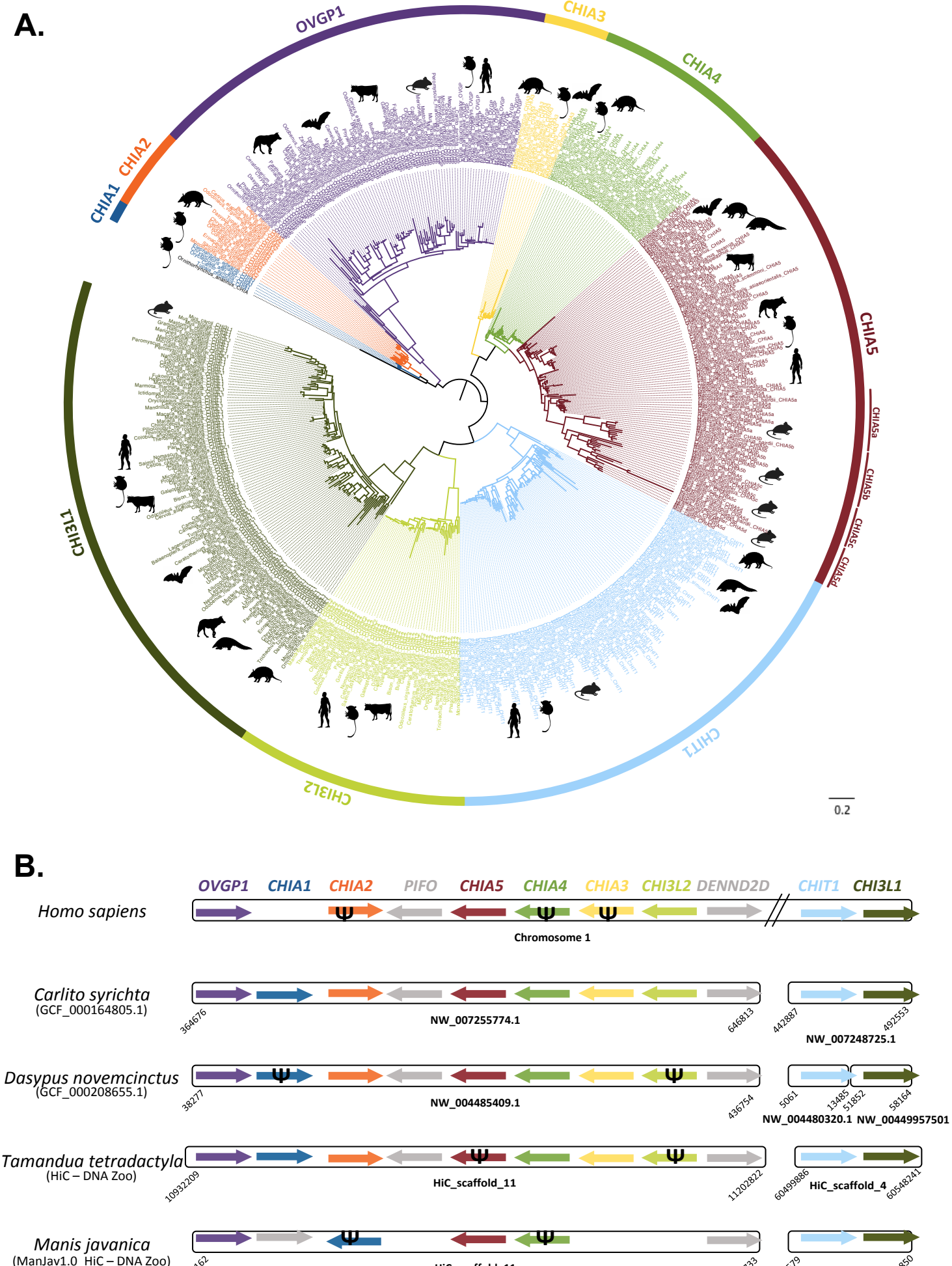
A.
OVGP1
CHIA3
CHIA4
CHIA1
CHIA2
CHIA5
CHIA5a
CHIA5b
CHIA5c
CHIA5d
CHI3L1
CHI3L2
CHIT1
0.2
B.
OVGP1 CHIA1 CHIA2 PIFO CHIA5 CHIA4 CHIA3 CHI3L2 DENND2D CHIT1 CHI3L1
Homo sapiens
Chromosome 1
Carlito syrichta
(GCF_000164805.1)
364676
NW_007255774.1
646813
442887
492553
NW_007248725.1
Dasypus novemcinctus
(GCF_000208655.1)
38277
NW_004485409.1
436754
5061
13485
51852
58164
NW_004480320.1
NW_00449957501
Tamandua tetradactyla
(HiC – DNA Zoo)
10932209
HiC_scaffold_11
11202822
60499886
HiC_scaffold_4
60548241
Manis javanica
(ManJav1.0_HiC – DNA Zoo)
94884162
HiC_scaffold_11
95065733
4626579
HiC_scaffold_3
4663850

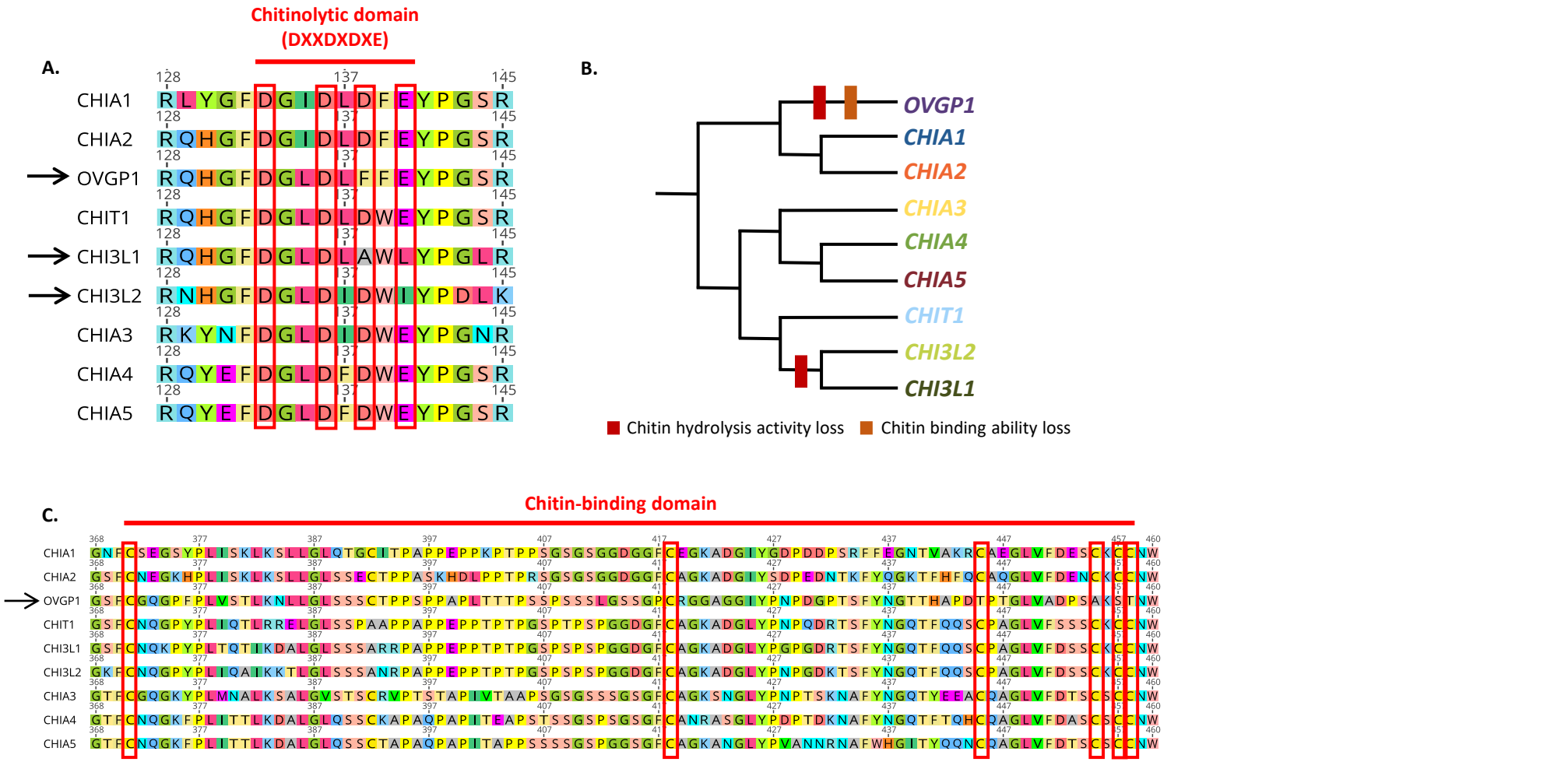
Chitinolytic domain
(DXXDXDXE)
A.
CHIA1
CHIA2
OVGP1
CHIT1
CHI3L1
CHI3L2
CHIA3
CHIA4
CHIA5
B.
OVGP1
CHIA1
CHIA2
CHIA3
CHIA4
CHIA5
CHIT1
CHI3L2
CHI3L1
Chitin hydrolysis activity loss
Chitin binding ability loss
Chitin-binding domain
C.
CHIA1
CHIA2
OVGP1
CHIT1
CHI3L1
CHI3L2
CHIA3
CHIA4
CHIA5

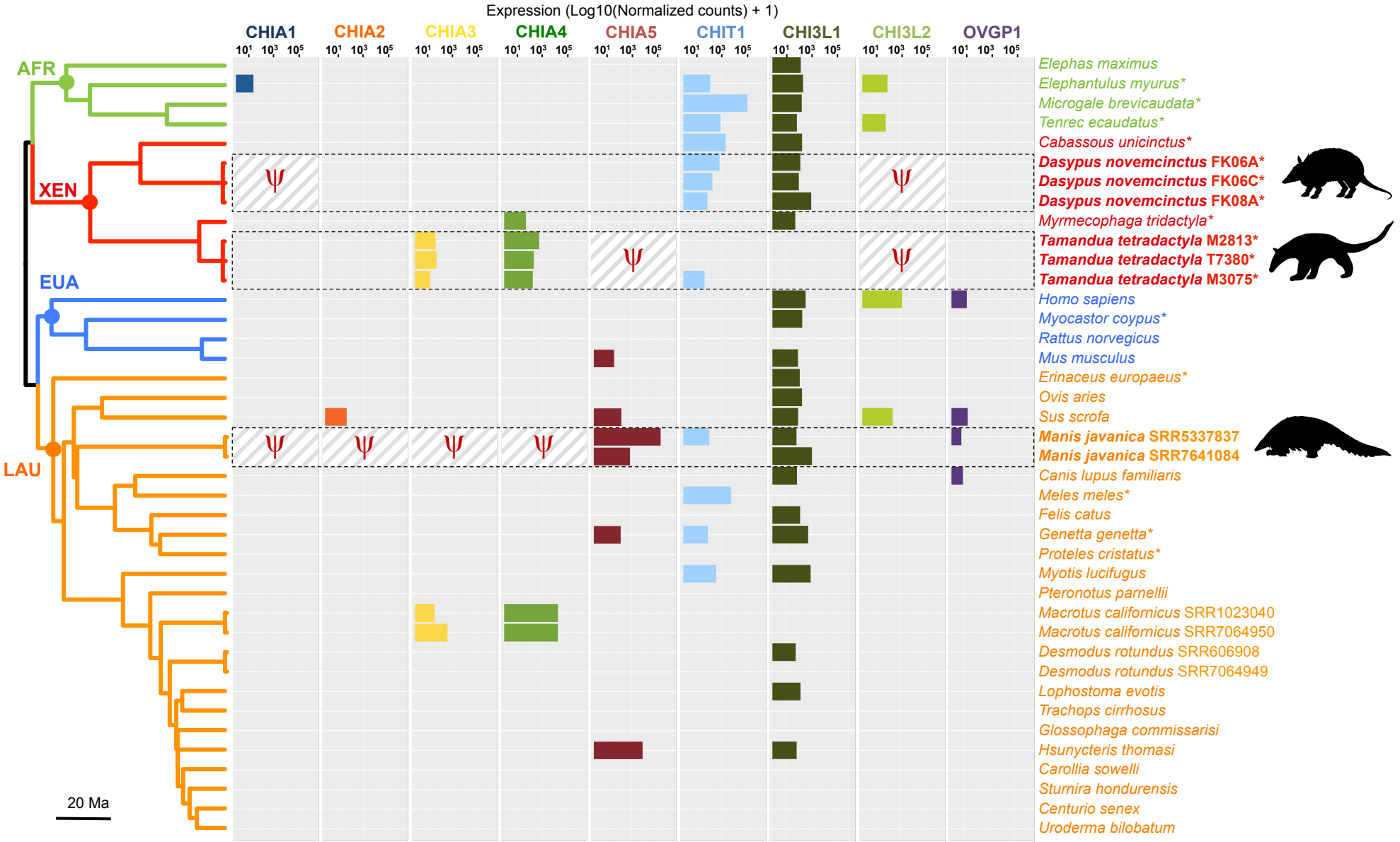
Expression (Log10(Normalized counts) + 1)
CHIA1
CHIA2
CHIA3
CHIA4
CHIA5
CHIT1
CHI3L1
CHI3L2
OVGP1
10^1 10^3 10^5
AFR
XEN
EUA
LAU
20 Ma
Elephas maximus
Elephantulus myurus*
Microgale brevicaudata*
Tenrec ecaudatus*
Cabassous unicinctus*
Dasypus novemcinctus FK06A*
Dasypus novemcinctus FK06C*
Dasypus novemcinctus FK08A*
Myrmecophaga tridactyla*
Tamandua tetradactyla M2813*
Tamandua tetradactyla T7380*
Tamandua tetradactyla M3075*
Homo sapiens
Myocastor coypus*
Rattus norvegicus
Mus musculus
Erinaceus europaeus*
Ovis aries
Sus scrofa
Manis javanica SRR5337837
Manis javanica SRR7641084
Canis lupus familiaris
Meles meles*
Felis catus
Genetta genetta*
Proteles cristatus*
Myotis lucifugus
Pteronotus parnellii
Macrotus californicus SRR1023040
Macrotus californicus SRR7064950
Desmodus rotundus SRR606908
Desmodus rotundus SRR7064949
Lophostoma evotis
Trachops cirrhosus
Glossophaga commissarisi
Hsunycteris thomasi
Carollia sowelli
Sturnira hondurensis
Centurio senex
Uroderma bilobatum

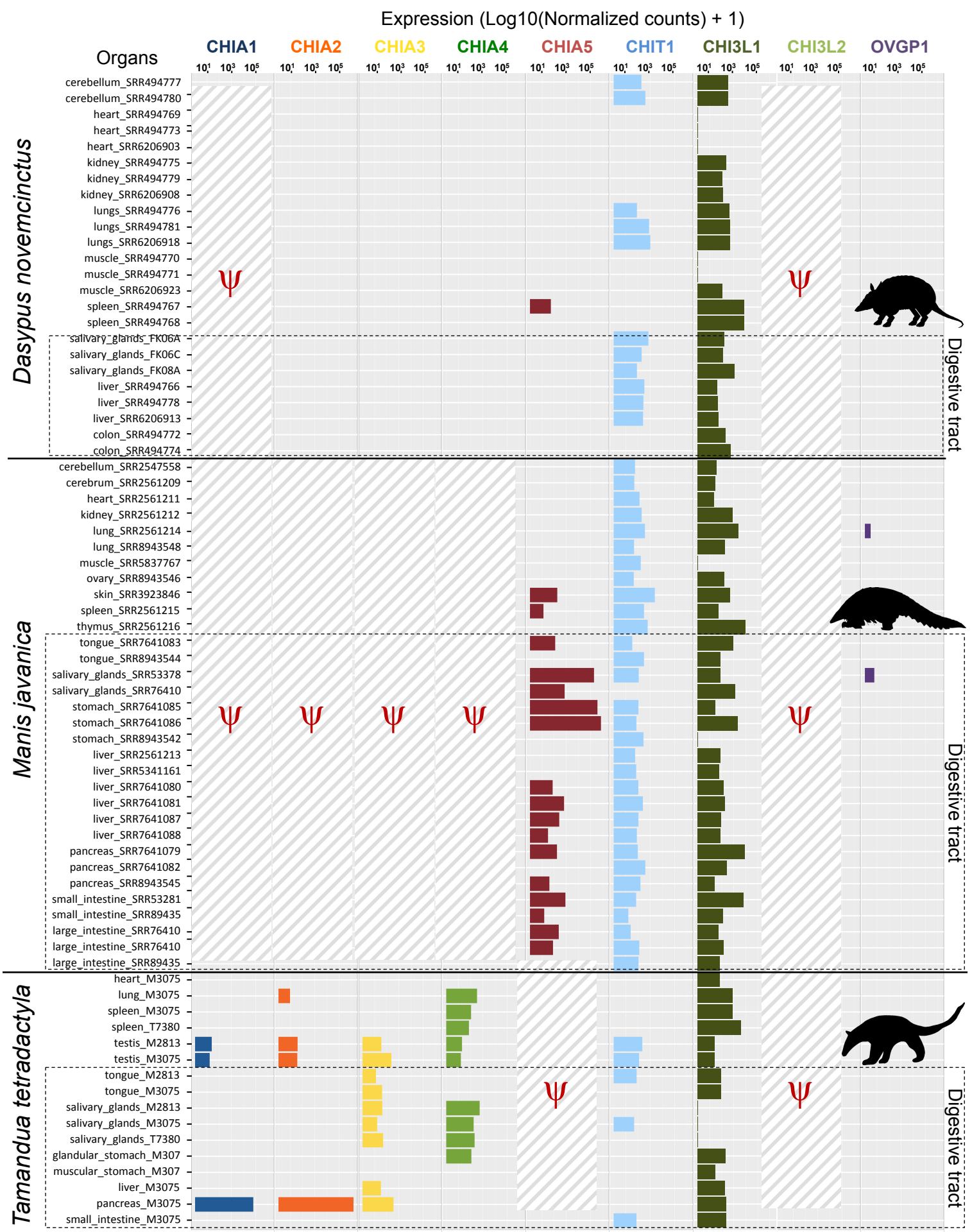
Expression (Log10(Normalized counts) + 1)
Organs
CHIA1
CHIA2
CHIA3
CHIA4
CHIA5
CHIT1
CHI3L1
CHI3L2
OVGP1
10^1 10^3 10^5
Dasypus novemcinctus
cerebellum_SRR494777
cerebellum_SRR494780
heart_SRR494769
heart_SRR494773
heart_SRR6206903
kidney_SRR494775
kidney_SRR494779
kidney_SRR6206908
lungs_SRR494776
lungs_SRR494781
lungs_SRR6206918
muscle_SRR494770
muscle_SRR494771
muscle_SRR6206923
spleen_SRR494767
spleen_SRR494768
salivary_glands_FK06A
salivary_glands_FK06C
salivary_glands_FK08A
liver_SRR494766
liver_SRR494778
liver_SRR6206913
colon_SRR494772
colon_SRR494774
Digestive tract
Manis javanica
cerebellum_SRR2547558
cerebrum_SRR2561209
heart_SRR2561211
kidney_SRR2561212
lung_SRR2561214
lung_SRR8943548
muscle_SRR5837767
ovary_SRR8943546
skin_SRR3923846
spleen_SRR2561215
thymus_SRR2561216
tongue_SRR7641083
tongue_SRR8943544
salivary_glands_SRR53378
salivary_glands_SRR76410
stomach_SRR7641085
stomach_SRR7641086
stomach_SRR8943542
liver_SRR2561213
liver_SRR5341161
liver_SRR7641080
liver_SRR7641081
liver_SRR7641087
liver_SRR7641088
pancreas_SRR7641079
pancreas_SRR7641082
pancreas_SRR8943545
small_intestine_SRR53281
small_intestine_SRR89435
large_intestine_SRR76410
large_intestine_SRR76410
large_intestine_SRR89435
Digestive tract
Tamandua tetradactyla
heart_M3075
lung_M3075
spleen_M3075
spleen_T7380
testis_M2813
testis_M3075
tongue_M2813
tongue_M3075
salivary_glands_M2813
salivary_glands_M3075
salivary_glands_T7380
glandular_stomach_M307
muscular_stomach_M307
liver_M3075
pancreas_M3075
small_intestine_M3075
Digestive tract